MEIOTIC CROSSOVER PATTERNING IN THE ABSENCE OF ATR

Morgan McNeil Brady

A dissertation submitted to the faculty at the University of North Carolina at Chapel Hill in partial fulfillment of the requirements for the degree of Doctor of Philosophy in the Curriculum in Genetics and Molecular Biology in the School of Medicine.

Chapel Hill
2017

Approved by:

Jeff Sekelsky

Dale Ramsden

Daniel McKay

Frank Conlon

Michael Jarstfer

ABSTRACT

Morgan McNeil Brady: Meiotic Crossover Patterning in the Absence of ATR
(Under the direction of Jeff Sekelsky)

Meiotic crossovers must be properly patterned to ensure accurate disjunction of homologous chromosomes during meiosis I. Disruption of the spatial distribution of crossovers can lead to nondisjunction, aneuploidy, gamete dysfunction, miscarriage, or birth defects. One of the earliest identified genes involved proper crossover patterning is *mei-41*, which encodes the *Drosophila* ortholog of the checkpoint kinase ATR. Although analysis of hypomorphic mutants suggested the existence of crossover patterning defects, it has not been possible to assess patterning in *mei-41* null mutants due to maternal-effect embryonic lethality. To overcome this lethality, we constructed *mei-41* null mutants in which we expressed wild-type Mei-41 in the germline after completion of meiotic recombination, allowing embryos to survive. We find that crossovers are decreased to about one third of wild-type levels, but the reduction is not uniform, being less severe in the proximal regions of *2L* than in distal *2L* or on the *X* chromosome. None of the crossovers formed in the absence of Mei-41 require Mei-9, the presumptive meiotic resolvase, suggesting that Mei-41 functions everywhere along the arm, despite the differential effects of crossover frequency. Interference appears to be significantly reduced or absent in *mei-41* mutants, but the reduction in crossover density in centromere-proximal regions is largely intact. We propose that crossover patterning is achieved in a stepwise manner, with suppression related to proximity to the centromere

happening prior to crossover designation and interference. In this model, Mei-41 is essential after the centromere effect is established but before crossover designation and interference occur.

To my parents, Joyce and Ted, my brother, David, and my partner, Matt,
for their unconditional love and support.

ACKNOWLEDGMENTS

Thank you first and foremost to my advisor, Dr. Jeff Sekelsky. His mentorship, respect, and humor fostered a nurturing and intellectually stimulating work environment for this gently-used graduate student, all of which was invaluable to my graduate career. I am also indebted to my committee, Dr. Frank Conlon, Dr. Mike Jarstfer, Dr. Dan McKay, and Dr. Dale Ramsden for their scientific (and philosophical!) advice and insight regarding my project and career. I would also like to thank my undergraduate research mentor and advisor, Dr. Judith Thorn, for her knowledge and support that ultimately guided me to graduate school at UNC.

Thank you to all my labmates and co-workers, past and present, for your genuine enthusiasm, insightful ideas, friendship, and support. I am especially grateful to Susan Cheek, my *mei-41* partner-in-crime and fellow connoisseur of post-punk. I consider myself lucky to have worked with such brilliant, passionate, and empathetic people. And to my friends outside the lab and outside the university, your creativity, solidarity, and encouragement has always been inspiring and absurdly (but pleasantly) surreal.

TABLE OF CONTENTS

LIST OF FIGURES

LIST OF TABLES

LIST OF ABBREVIATIONS

ATM	Ataxia-telangiectasia mutated
ATR	ATM and Rad3-related
BF	beam-film
BS	Bloom syndrome
CO	crossover
dHJ	double Holliday junction
DDR	DNA damage repair
DSB	double-strand break
DSBR	double-strand break repair
HJ	Holliday junction
HR	homologous recombination
JM	joint molecule
MBT	midblastula transition
NC	nuclear cycle
NCO	non-crossover
NER	nucleotide excision repair
SC	synaptonemal complex
SDSA	synthesis-dependent strand annealing
SEI	single end invasion
ssDSB	single-stranded DSB

CHAPTER 1

MEIOTIC CROSSOVER PATTERNING AND THE TWO-PATHWAY PARADIGM

Meiosis is a specialized cellular process, required for both genetic diversity and the accurate segregation of chromosomes within sexually reproducing organisms. During gametogenesis, each homologous chromosome undergoes one round of DNA synthesis, thus creating sister chromatids and doubling the DNA content of the germ cell. This genomic doubling is followed by two rounds of cellular division (first separating the homologs, then separating the sisters) resulting in haploid gametes each containing half the parental chromosome content of the original diploid cell. An additional function of the meiotic program is the process of meiotic recombination, an event that occurs prior to the first meiotic division during prophase I. Meiotic recombination is deliberately initiated by double-strand breaks (DSB), whose lesions are resolved by the evolutionarily conserved homologous recombination (HR) repair pathway. Products resulting from successful meiotic HR recombination are of two varieties: crossovers (CO), in which there is a reciprocal exchange of homologous chromosomes distal to the site of recombination, and non-crossovers (NCO), in which DNA flanking the recombination site remains unchanged (reviewed in Kohl and Sekelsky 2013; reviewed in Cooper *et al.* 2016).

Unlike meiotic cells, DSBs in mitotic cells are the result of exogenous or endogenous sources of DNA damage, and can therefore be deleterious if not properly repaired (reviewed in Symington and Gautier 2011). Although many DNA damage

repair (DDR) proteins present during mitotic repair and meiotic recombination are the same, the meiotic program utilizes additional proteins specific to meiosis, leading to the proposal that meiotic recombination evolved from mitotic repair (reviewed in Marcon and Moens 2005). This theory is further supported by the existence of two meiotic pathways, one utilizing meiotic-specific double-strand break repair (DSBR) mechanisms to preferentially create COs, while the other shares more similarities with mitotic DSBR and results predominantly in NCOs (reviewed in Kohl and Sekelsky 2013).

To compare, mitotic cells avoid COs between homologous chromosomes, and subsequent DNA repair of DSBs utilizes the sister chromatid as a template to prevent loss of heterozygosity. However, the meiotic program deliberately induces DSBs by the conserved topoisomerase-like endonuclease Spo11 (Bergerat *et al.* 1997, Keeney *et al.* 1997), enforcing COs between homologous chromosomes in order to obtain genetic diversity and accurate segregation of homologous chromosomes during anaphase I.

Moreover, meiosis developed several mechanisms of strict temporal and spatial control to establish the optimal location and number of meiotic COs throughout the recombination process. First, CO assurance is an inter-chromosomal phenomenon that ensures each homolog pair receives at least one CO, thus creating not only genetic diversity, but also creating tension needed on the meiotic spindle for chromosome stability. Second, CO interference is an intra-chromosomal phenomenon resulting in the even spacing of COs along the chromosome arm by inhibiting additional COs in regions flanking CO precursors. Third, while crossover assurance and interference denote the minimum and maximum number of crossovers per meiosis, crossover homeostasis acts as a buffer to ensure crossover number remains static per species, despite increases or

decreases in meiotic DSBs (reviewed in Wang *et al.* 2015). Lastly, the centromere effect is an intra-chromosomal phenomenon that suppresses CO formation at the euchromatin proximal to the centromere (reviewed in Choo 1998). Together, these additions to the meiotic program prevent loss of heterozygosity, aneuploidy, and other forms of genomic catastrophe that may otherwise lead to cell death, miscarriage, or birth defects (Koehler *et al.* 1996; Lamb *et al.* 1996; reviewed in Nagaoka *et al.* 2012).

Unfortunately, many mechanisms of CO control remain elusive. Perturbing one mechanism often alters another, confounding resulting data and suggesting that certain phenomena are the result of a single patterning process (reviewed in Hunter *et al.* 2015). Additionally, the existence of a 'back-up' Class II meiotic pathway makes genetic approaches difficult due to the number of genes that must be mutated to pinpoint active participants within these mechanisms. Despite this, using a molecular genetic approach, we can exploit the two-pathway paradigm to determine when different CO patterning phenomena are established based on when class switching occurs.

Mitotic versus Meiotic Division

While many mechanisms of mitosis and meiosis II are quite similar, mechanisms governing meiosis I impose additional requirements to successfully complete meiotic recombination. Mitotic cell division is the result of an equational division, wherein homologous chromosomes from each parent are replicated and, following cytokinesis, each daughter cell contains the same number of chromosomes as the mother cell. Similarly, meiosis II is also an equational division, where the number of each chromatids in the resulting daughter cells is the same as in the original mother cell, with the exception that up to half of these chromatids are no longer identical due to earlier

meiotic recombination (reviewed in Marcon and Moens 2005, reviewed in Hunter *et al.* 2015).

Alternatively, meiosis I is a reductional division, yielding a haploid genome from a diploid genome. Following DNA replication of each parental homolog, meiosis I reduces the two sets of paired, homologous chromosomes to one set per daughter cell following cytokinesis. Additionally, homologous chromosomes in meiosis I rely on physical linkages between each other via CO formation (seen cytologically as chiasma), resulting in the creation of a bivalent (Owen 1949). Tension created via this physical linkage facilitates the alignment of homologs on the metaphase plate, resulting in their proper disjunction during anaphase I (McKim 1993). Therefore, CO formation and resolution are essential in meiosis I not only for genetic diversity, but also for proper homolog disjunction (reviewed in Miller *et al.* 2013, reviewed in Andersen and Sekelsky 2010).

Meiotic CO and NCO Resolution

Current models of meiotic recombination are based off the 1964 model proposed by Robin Holliday (Holliday 1964), though the model has gone through many revisions over the last 50 years. Most current understanding of meiotic recombination is derived from studies at the molecular level in *S. cerevisiae* (Schwacha and Kleckner 1994, Hunter and Kleckner 2001) (Figure 1.1). Induction of meiotic DSBs is carried out by the Spo11 transesterase, forming a protein-DNA complex at both ends of the break (Keeney *et al.* 1997; reviewed in Keeney 2008). Spo11 is removed via single-stranded endonucleolytic cleavage by Mre11 and Sae2. Resulting nicks are resected in a bidirectional manner by Mre11 and Exo1, generating the 3' overhangs required for

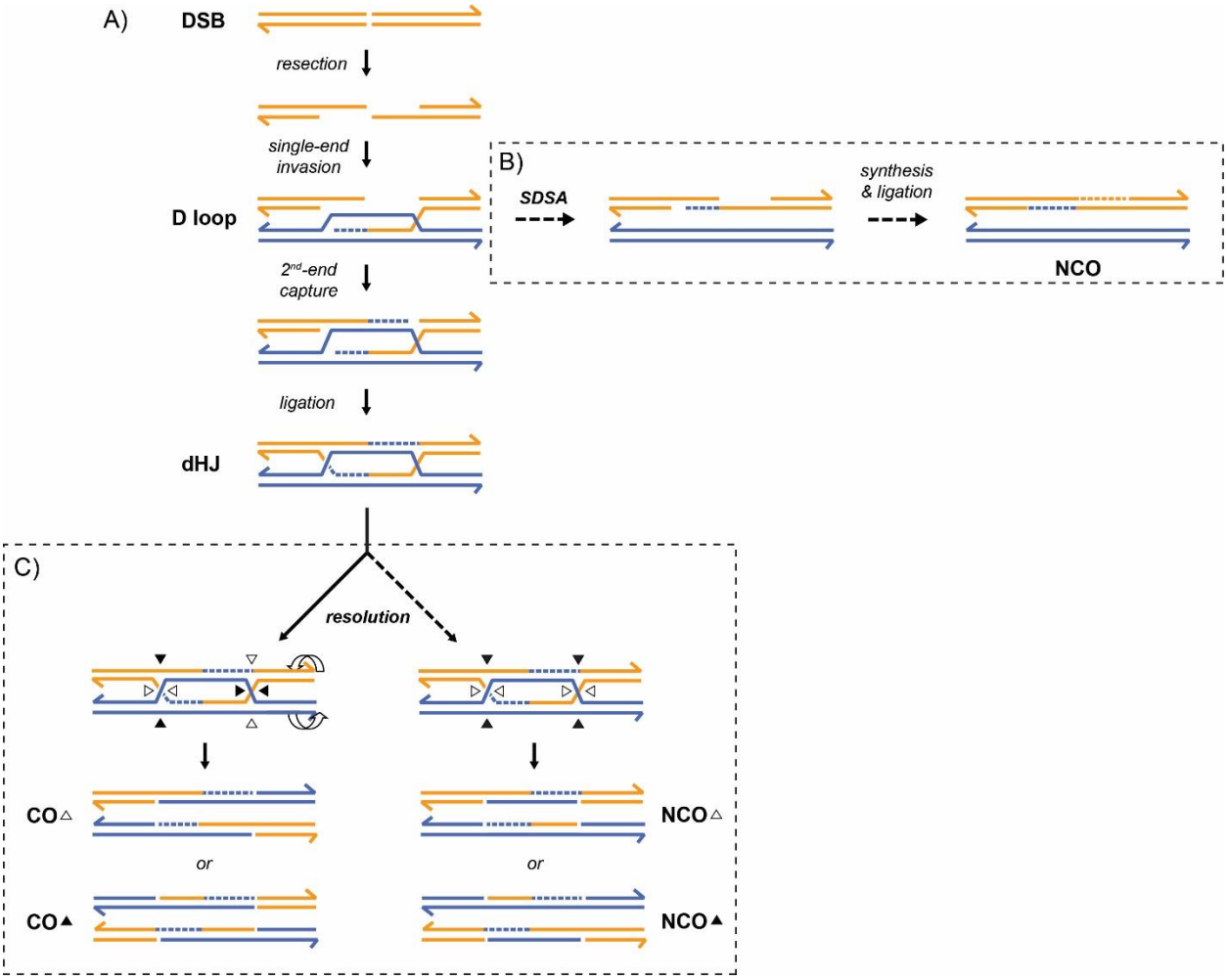

Figure 1.1. Model for crossover versus non-crossover designation. (A) DSB resection results in D loop formation, a joint molecule that can be disassociated via Sgs1-mediated SDSA into an NCO (B). Alternatively, the D loop can be stabilized via second-end capture to form an SEI, which is then ligated to create a dHJ. From here, dHJs are preferentially resolved into a COs (solid black line) via endonucleases in one of two manners, though occasionally NCOs occur (dashed black lines) (C). Nick orientations are denoted as black triangles or white triangles, with resulting outcomes labeled below.

homolog invasion (Neale *et al.* 2005; Manfrini *et al.* 2010; reviewed in Andersen and Sekelsky 2010; Garcia *et al.* 2011).

The first joint molecule (JM) is formed when one 3' overhang preferentially invades the homolog (as opposed to the sister chromatid) via the meiosis-specific *S. cerevisiae* Rad51 homolog Dmc1 to create a D loop (Figure 1.1A) (Schwacha and

Kleckner 1994; reviewed in Shinohara and Shinohara 2004). The resulting D loop can be disassembled via the BLM homolog, Sgs1, to form an NCO via synthesis dependent strand annealing (SDSA) (Figure 1.1B) (Allers and Lichten 2001; reviewed in Hatkevich and Sekelsky 2017). Alternatively, second-end capture can occur, where the D loop is 'captured' by the 3' overhang of the homolog to form a stable single-end invasion intermediate (SEI) (Hunter and Kleckner 2001). As the primary product of interhomolog strand exchange, SEIs can then be ligated to form a double-Holliday junction (dHJ), from which COs are preferentially formed by meiotic resolvases Mlh1 and Mlh3 (Figure 1.1C) (Allers and Lichten, 2001; Hunter and Kleckner 2001; Zakharyevich *et* al. 2012; reviewed in Manhart and Alani 2016).

Crossover Control

While the addition of specific meiotic proteins contributes to proper crossover formation, chromosome segregation, and genetic diversity, these proteins and their interactions must be tightly regulated within the meiotic program. Although there are a greater number of DSBs created during meiotic prophase I, only a few select sites become CO competent, with the remaining recombinational intermediates resolved into NCOs (reviewed in Wang *et al.* 2015). While the many of the exact mechanisms governing CO choice remain elusive, the establishment of proper CO patterning requires several meiotic phenomena under strict temporal and spatial control, both within each chromosome arm and between homologous chromosomes. This regulation ensures optimal CO formation that follows a consistent, repeatable number and distribution of COs along the arms of chromosomes in most species (reviewed in Hunter *et al.* 2015).

Crossover Assurance

Assurance was first described cytologically in 1932, when Darlington and Dark noticed each homologous chromosome pair of the male grasshopper *Stenobothrus parallelus* contained at least one chiasma (Darlington and Dark 1932). The presence of at least one chiasma between each homologous chromosome pair was later termed the obligate chiasma, or obligate crossover, and its presence is required for proper disjunction between the homologous chromosomes during meiosis I (Owen 1949).

Additionally, there is pressure within the meiotic program to establish COs between homologs as opposed to sister chromatids (as would be the case during potentially deleterious somatic recombination events) (Kadyk and Hartwell 1992, Byzmek *et al.* 2010). Previous studies in *S. cerevisiae* show that the meiosis-specific strand exchange protein Dmc1, together with Rad51, promote interhomolog recombination (Cloud *et al.* 2012). However, *Drosophila* lacks a Dmc1 homolog, potentially attributable to the fact that, unlike yeast or mammals, homolog synapsis via the synaptonemal complex (SC) occurs before Spo11/Mei-W68 meiotic DSB induction (Jang *et al.* 2003). Taken together, CO assurance ensures proper disjunction of homologous chromosomes while increasing genetic diversity via homologous recombination.

Crossover Interference

Sturtevant, while constructing the first genetic map for *Drosophila*, noticed that paired homologous chromosome arms containing more than one CO were widely spaced apart (Sturtevant 1913), implicating a phenomenon in which CO formation at one site inhibits additional CO formation within flanking intervals. While the mechanism

of CO interference is the subject of intense study, the beam-film (BF) model suggests that the probability of these additional COs is diminished at intervals surrounding DSBs already committed to crossing over (crossover precursors) via the reduction of mechanical stress along chromosome axes (Zhang *et al.* 2014). Within the BF model, CO designation occurs when accumulated mechanical stress, most likely along the chromosome axis, is relieved at a meiotically-induced DSB site. This stress relief is redistributed along the chromosome arm, preventing flanking DSBs from attaining the stress required for CO designation, generating CO interference (reviewed in Berchowitz and Copenhaver 2010; reviewed in Zhang *et al.* 2014).

Crossover Homeostasis

While CO assurance and CO interference delimit the lower and upper levels of CO formation per species, CO homeostasis acts as a buffering process to ensure that any increase or decrease of CO precursors does not disrupt the establishment of proper meiotic patterning. Within the context of the BF model, high densities of CO precursors are more affected by spreading interference, while low densities are less affected (Zhang *et al.* 2014, reviewed in Zhang *et al.* 2014). Therefore, despite any increases or decreases in meiotically-induced DSBs, CO homeostasis regulates the number of COs formed, thereby avoiding any excess or deficiency in CO formation and maintaining proper CO patterning (reviewed in Wang 2015). Due to this plastic interplay between CO assurance, CO interference, and CO patterning, all three appear to be the result of a single patterning process (reviewed in Kleckner *et al.* 2004; reviewed in Wang *et al.* 2015).

The Centromere Effect

Unlike previously mentioned CO control phenomena, the centromere effect appears to be governed by alternative mechanisms. The centromere effect was first described in the 1930's as a phenomenon in which meiotic recombination occurs at a significantly lower frequency nearer to the centromere than elsewhere along the arm of the chromosome (Beadle 1932; Sturtevant and Beadle 1936; Mather 1939). Although the pericentromeric region is primarily composed of heterochromatin, it is unlikely to be the cause. Heterochromatin itself undergoes minimal recombination when interrupted by small euchromatic regions (Brown 1940, Roberts 1965), but wholly heterochromatic regions show no meiotic recombination (Atwood 1969). Additionally, experiments in *D. virilis,* wherein heterochromatin proximal to the centromere of chromosome 5 was translocated to a distal region on chromosome 3L, again resulted in low heterochromatic recombination frequency (0.16%), though this heterochromatin contained small amounts of euchromatin flanking the breakpoints. Interestingly, euchromatin flanking the translocated heterochromatin showed wild-type recombination frequencies (Baker 1958). However, when pericentromic heterochromatin is deleted in *Drosophila*, meiotic recombination in pericentromeric euchromatin remains suppressed, with greater CO decreases in euchromatin correlating with larger heterochromatic deletions. This suggests that the centromere itself is the source of crossover inhibition, as the closer euchromatin gets to the centromere, the greater the reduction in COs (Yamamoto and Miklos 1977; reviewed in Choo 1998).

Recent experiments analyzing the role of higher-order chromatin structure at the centromere implicates the kinetochore as a major player in inhibiting pericentromeric

recombination. The Ctf19/CCAN kinetochore subcomplex in *S. cerevisiae* inhibits initial meiotic breaks and suppresses CO formation in these areas via enrichment of cohesin, a protein complex formed between sister chromatids which promotes inter-sister recombination (Vincenten *et al.* 2015). Together, these data suggest that DSBs formed near the centromere undergo recombination with the sister chromatid as opposed to the homolog, reminiscent of mitotic DSBR. This is somewhat at odds with meiotic *Drosophila* DSB landscapes, where DSBs levels (and thus, potential CO precursors) are uniformly distributed along each arm, including pericentromeric euchromatin (Comeron *et al.* 2012). Further research into centromeric chromatin and its associated proteins is needed to establish an appropriate mechanism for the centromere effect in animals with large, complex centromeres.

The Two-Pathway Paradigm

In addition to CO control mechanisms, the meiotic program of many species has an alternate CO-generating system in place (reviewed in Kohl and Sekelsky 2013). In *S. cerevisiae*, the loss of meiosis-specific ZMM proteins Msh4 and Msh5 results in a 50%-70% reduction of CO formation (Ross-Macdonald and Roeder 1994; Hollingsworth *et al.* 1995), while the loss of these proteins in *C. elegans* abolished COs entirely (Zalevsky *et al.* 1999 and Kelly *et al.* 2000), leading to the hypothesis that a second pathway was responsible for the remaining COs formed in *S. cerevisiae*. Alternatively, *S. pombe* relies exclusively on the Mus81-Mms4 resolvase for all COs and completely lacks Msh4-Msh5 orthologs (reviewed in Villeneuve and Hillers 2001; Smith *et al.* 2003). Subsequent experiments in both *S. cerevisiae* and *A. thaliana* lacking both Msh4-Msh5 and Mus81-Mms4 displayed a severe, synthetic reduction in COs than Msh4-Msh5 or

Mus81-Mms4 mutants alone (de los Santos *et al.* 2003; Berchowitz *et al.* 2007), providing additional evidence that two CO pathways are present in these species.

Current models focus heavily on results from *S. cerevisiae*. These models place COs dependent on both Msh4-Msh5, which is believed to stabilize recombination intermediates and prevent disassembly by Sgs1, and the Mlh1-Mlh3 endonuclease into the Class I pathway. Alternatively, COs generated through the Class II pathway require the Mus81-Mms4 resolvase (Zakharyevich *et al.* 2012, reviewed in Manhart and Alani 2016, reviewed in Hatkevich and Sekelsky 2017). More intriguing is the fact that the Class I pathway relies heavily on meiosis-specific DSBR mechanisms. These mechanisms require the anti-CO BLM ortholog Sgs1 and preferentially generate interfering COs following dHJ resolution. Alternatively, Class II CO generation is more similar to *mitotic* DSBR. Prior to dHJ formation, NCOs are preferentially generated via SDSA; however, following dHJ resolution, any remaining DSBs are equally resolved into NCOs or non-interfering COs (Copenhaver *et al.* 2002, De Muyt *et al.* 2012, Zakharyevich *et al.* 2012, reviewed in Kohl and Sekelsky 2013).

Drosophila lack Msh4-Msh5 in favor of the mei-MCM protein complex (Kohl *et al.* 2012). Additionally, flies utilize the nucleotide excision repair (NER) endonuclease XPF ortholog Mei-9 to resolve meiotic crossovers (Sekelsky *et al.* 1995). Entry into the Class I pathway relies on the human BLM ortholog, encoded by *Blm* in *Drosophila*, as CO patterning is completely lost in *Blm* mutants (Hatkevich *et al.* 2017). Alternatively, while there is a 90% reduction in CO formation in *mei-9* mutants, CO patterning remains intact and may rely on mitotic-like HJ resolvases, such as Mus81/MUS81,

Mus312/SLX4, and Gen/GEN1, to carry out meiotic recombination (Andersen *et al.* 2011; Hatkevich *et al.* 2017).

Taken together, these data suggest that the Class I pathway is not only the predominant pathway for preferentially generating COs, establishing CO control, and preventing NDJ in these two species, but as hypothesized by Marcon and Moens, may have evolved from mitotic DSBR (Marcon and Moens 2005). The existence of the mitotic-like Class II pathway (or pathways that fall outside the canonical meiotic program) may therefore act as a backup for residual CO generation in the absence of Class I proteins (reviewed in Kohl and Sekelsky 2013).

Meiosis in *Drosophila melanogaster*

Drosophila melanogaster has been used in genetic analysis for over 100 years, first in 1901 by William Castle, but popularized soon after by Thomas Hunt Morgan while studying genetic linkage and crossing over (reviewed in Jennings 2011; reviewed in Hawley 1993). Its historical longevity as a model organism is not unwarranted, as it an exceptional tool for the study of a variety of biological processes, particularly meiosis. On a logistical level, *Drosophila* are easy to maintain, have a short reproductive life-span, numerous phenotypic markers, and a single female is capable of producing hundreds of progeny for further analysis (Ashburner 2005). Genetically, only females undergo meiotic recombination, thus aiding in the study of meiotic recombination as all events must come from the mother (Morgan 1912); moreover, *Drosophila* have a high tolerance for nondisjunction on the *X* and *4* chromosomes (Ashburner 2005), serving as an easily detectable phenotype for mutants perturbing various aspects of CO control when appropriately marked. Histologically, the controlled,

temporal procession of the oocyte moving through the egg chambers within female ovariole allows for easy staging and staining of meiotic proteins of interest (Nagoshi 2004); though the early, pre-blastoderm embryo can prove difficult for microscopy due to its 3-dimensionality and high, opaque yolk content (personal observations).

Meiotic Recombination in the Drosophila *Germarium*

Drosophila females have two ovaries, each containing 15-20 ovarioles (Spradling 1993, reviewed in Ables 2015). Each ovariole resembles a chain-like sequence of egg chambers and is divided into two major sections: the anterior germarium (where meiotic recombination occurs, termed stage 1) and the posterior vitellarium (where oocyte growth occurs, containing stages 2-14). (Von Stetina and Orr-Weaver 2011).

The germarium itself is divided into 4 separate regions: region 1 (mitotic/pre-meiotic) and regions 2A, 2B, and 3 (meiotic) (Figure 1.2). Within pre-meiotic region 1, germline stem cells at the anterior end of the germarium divide to produce a daughter stem cell and cystoblast (Nagoshi 2004, reviewed in Lake and Hawley 2012). The cystoblast undergoes four rounds of mitotic replication to produce an interconnected 16-cell cyst (Xie 2013). Cohesin proteins binding sister chromatids together become enriched around the centromeres within the 8-cell cyst, but SC proteins binding homologs together do not appear until early in region 2A, during zygotene. Early pachytene also occurs in region 2A, where two pro-oocytes complete SC formation and undergo programmed DSBs, followed by a decrease in DSBs in region 2B. By mid-pachytene in region 3, almost no DSBs remain, suggesting meiotic recombination has either resolved DSBs into NCOs or formed COs. Additionally, the pro-oocyte not chosen to become the oocyte disassembles its SC and, like the other 14 cells within the germline cyst, becomes a nurse cell

(Ashburner 2005; reviewed in Lake and Hawley 2012). All further meiotic development occurs within the vitellarium (Spradling 1993).

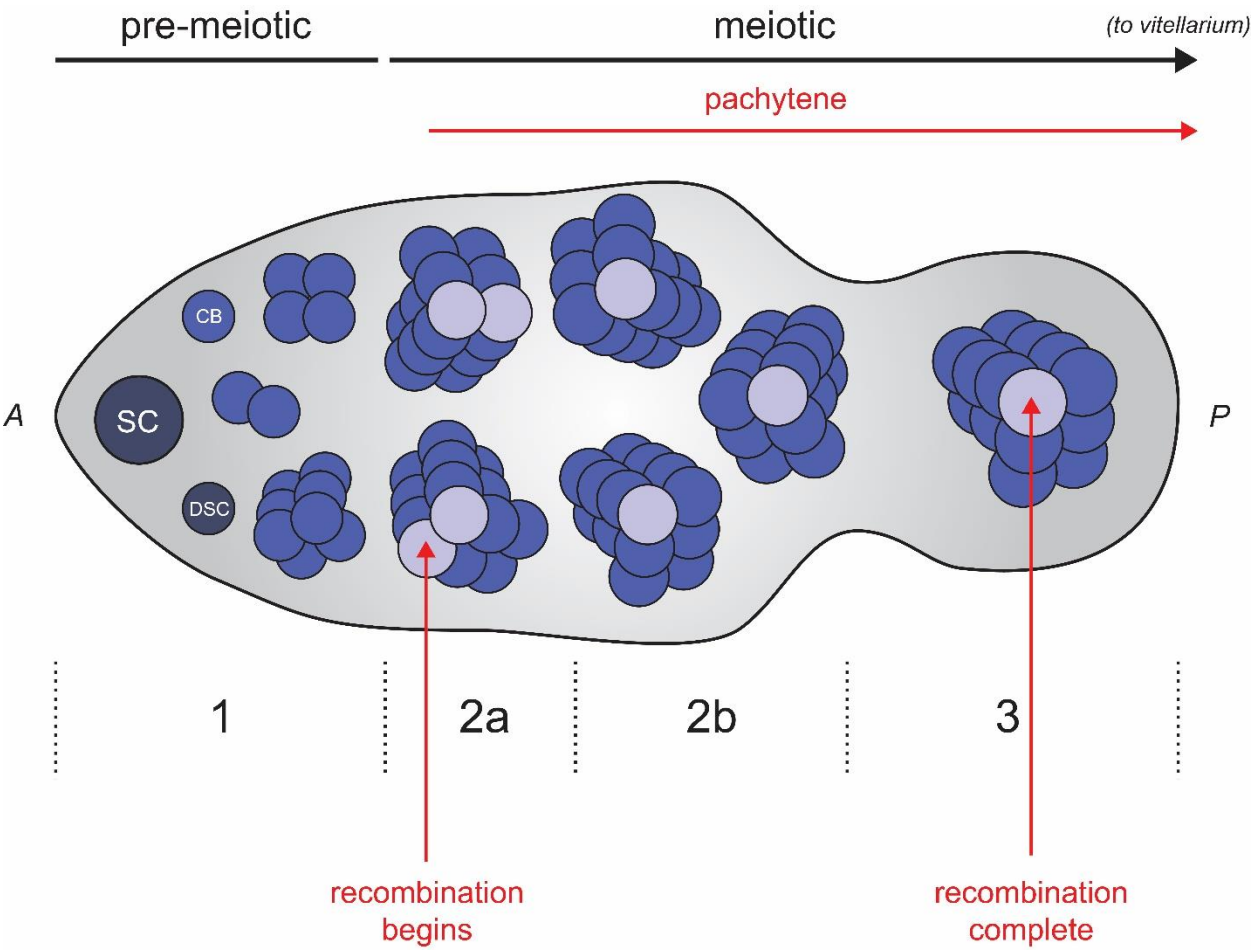

Figure 1.2. Staging of meiotic recombination in the *Drosophila* germarium. The *Drosophila* germarium is divided into 4 stages, with mitotic division occurring at stage 1 and early prophase in MI occurring at stages 2a, 2b, and 3. At the anterior end (A) of the germarium, stem cells (SC, gray) asymmetrically divide to form a daughter stem cell (DSC, gray) or a cystoblast (CB, blue). Following 4 rounds of mitotic division in stage 1, two pro-oocytes within the cystoblast are selected at stage 2a (light blue) while the rest become nurse cells (blue). Meiotic recombination begins within the pro-oocytes at early pachytene at stage 2a. Final oocyte selection occurs at stage 2b (note one light blue cyst) and meiotic recombination is complete by region 3. All further meiotic development occurs within the vitellarium, posterior (P) to the germarium in the female fly.

Exploiting Crossover Control in Context of the Two-Pathway Paradigm

Drosophila is an excellent model organism in which to study meiotic crossover control in context of the two-pathway paradigm. While many of the mechanisms of meiotic CO formation have been elucidated in *S. cerevisiae,* recent work demonstrates that many proteins and pathways are conserved in *Drosophila* (reviewed in Kohl and Sekelsky 2013; Hatkevich *et al. 2017*). Therefore, by exploiting our current knowledge regarding CO control formation within the canonical meiotic Class I pathway, we can use a molecular genetic approach to tease apart when CO control is established by observing CO patterning loss, indicative of a Class II (or alternative, mitotic-like) switch, in *Drosophila* mutants of interest. As most instances of meiotic NDJ are attributable to CO patterning loss during MI in both *Drosophila* and humans, as opposed to maternal age, understanding CO regulation may shed light on the origins of aneuploidy that often result in human miscarriage and trisomic syndromes (Lamb *et al.* 1996; Koehler *et al.* 1996).

CHAPTER 2

ATR AND THE *DROSOPHILA* ORTHOLOG MEI-41

Organisms have developed a complex response to DNA damage (DDR) caused by various genotoxic stressors to preserve genomic fidelity. The ability to sense DNA damage, signal cell-cycle arrest, and trigger either DNA repair or cellular apoptosis is highly dependent upon proteins within this network working in (near-perfect) concert with one another. ATR (ATM and Rad3-related), along with its fellow PI3K-related kinase ATM (Ataxia-telangiectasia mutated), are often the initial responders within this DDR network. While ATM responds to genotoxic DSBs, ATR responds to ssDSBs resulting from either resected DSBs or fork stalling (reviewed in Maréchal and Zhou 2013; reviewed in Cooper *et al.* 2014).

It is therefore not surprising that ATR has also been implicated in meiotic pathways, where genetic diversity and proper homolog segregation are dependent upon programmed DNA breaks. While not known as the ATR ortholog in 1972, *Drosophila mei-41* hypomorphs severely perturb CO patterning and homolog disjunction (Baker and Carpenter 1972). Additionally, co-opting ATR to suit the needs of the meiotic program may be expected in the context of the two-pathway paradigm, where mitotic DDR proteins take on specialized roles during prophase I to ensure accurate homolog recombination (reviewed in Kohl and Sekelsky 2013).

ATR Structure, Interactions, and Syndromes

Structurally, ATR is a serine/threonine protein kinase that belongs to the phosphatidylinositol-3-OH kinase (PI3K)-related protein family. Members within this family are large (2000-4000 amino acids) and share a well conserved C-terminus kinase domain responsible for substrate phosphorylation at serine/threonine residues preceding glutamine residues (SQ/TQ) sites (Bosotti *et al.* 2000). This PI-kinase domain is flanked by FAT/FATC domains, whose placement suggests FAT/FATC ensure proper function of the kinase domain via conformational interaction with each other (Bosotti *et al.* 2000, Sibanda *et al.* 2010). However, the majority of the protein is composed of flexible a-helical HEAT repeats at the N-terminus, several of which are involved in protein-protein interactions important for kinase function and regulation (Sibanda *et al.* 2010, and reviewed in Maréchal and Zou 2013). HEAT repeats are required for the recruitment of ATR to RPA-coated single stranded DSBs (ssDSB) via their interaction with the ATR activator protein ATRIP. Together with the 9-1-1 complex (RAD9/RAD1/HUS1), a PCNA-like DNA clamp, ATR phosphorylates a number of downstream targets involved in DDR, cell cycle arrest, and apoptosis (Ball *et al.* 2005; reviewed in Mordes and Cortez 2008; reviewed in MacQueen and Hochwagen 2011). Similar to PI3K-like kinases identified in other organisms, the *Drosophila* ortholog of ATR is encoded by *mei-41* and results in a large protein (2347 amino acids) containing the well-conserved C-terminus kinase domain flanked by predicted FAT/FATC accessory domains (Hari *et al.* 1995; Song *et al.* 2004).

To date, there are two well-characterized disease states found in humans who acquire mutations within the ATR gene. The first, Seckel syndrome-1 (SCKL1) is a rare,

autosomal-recessive loss-of-function disorder resulting in various ATR signaling cascade defects (Alderton *et al.* 2004). Patients therefore display heterogeneous phenotypes, including intellectual disabilities, microcephaly, proportional dwarfism, delayed intrauterine growth, and facial and central nervous system anomalies (O'Driscoll *et al.* 2003; Shanske *et al.* 1997; Alderton *et al.* 2004).

The second, familial cutaneous telangiectasia and cancer syndrome (CTCSF), is caused by an autosomal-dominant missense mutation within a well conserved FAT domain amino acid. Interestingly, this mutation does not reduce ATR expression following hydroxyurea exposure in fibroblasts, but instead leads to a decrease in the activity of the ATR substrate p53. Patients therefore show skin telangiectases and more than half developed malignancies, usually oropharyngeal cancer (Tanaka *et al.* 2012).

Mitotic Roles of Mei-41 in *Drosophila melanogaster*

Most organisms rely on the interplay between the ATR and ATM kinases to deal with DNA breaks in somatic cells. Downstream checkpoint mediators phosphorylated by these kinases, such as CHK1 and CHK2, are required for the activation of DDR and checkpoint response (reviewed in MacQueen and Hochwagen 2011). *Drosophila mei-41* encodes the ATR ortholog, which is required for the checkpoint response to unrepaired DSBs. Similarly, *Drosophila* orthologs of CHK1 and CHK2, encoded by *grapes* and *loki*, respectively, are required for Mei-41 dependent replication and DDR checkpoints (Su *et al.* 1999; Yu *et al.* 2000 Abdu *et al.* 2002; Masrouha *et al*. 2003; Brodsky *et al.* 2004; Jaklevic and Su 2004; Royou et al. 2005; LaRocque et al. 2007).

Mei-41, via its transducer Grapes, is required for delaying entry into mitosis following both IR and replication inhibition (Hari *et al.*, 1995; Sibon *et al.* 1999, Brodsky *et al.* 2000; Garner *et al.* 2001; Jaklevic and Su 2004). Additionally, Mei-41 is required for the repair of both widespread IR-induced DSBs and acute transposase-induced DSBs independent of cell cycle checkpoints, the latter of which affects repair via HR in the final steps of SDSA (Jaklevic and Su 2004; Oikemus *et al.* 2006; LaRocque *et al.* 2007). Larvae mutant for *mei-41* are also hypersensitive to nitrogen mustard, UV, and MMS (Baker *et al.* 1976; Boyd *et al.* 1976).

Homozygous null mutations of *mei-41* display maternal-effect embryonic lethality in the early embryo (Sibon *et al.* 1999). In *Drosophila*, early embryogenesis occurs via synchronous nuclear cycles (NC) in syncytium, with nuclei under the direction of maternally loaded cellular components rapidly oscillating between S phase and mitosis at the expense of G1 and G2 gap phases. While the first 10 nuclear cycles allow for the creation of a large number of undifferentiated multinuclei early in development, they lack DNA damage checkpoint mechanisms required to monitor genomic integrity that would otherwise occur at the G1/S and G2/M borders (Foe and Alberts 1983; reviewed in O'Farrell *et al.* 2004; reviewed in Duronio 2012). It is therefore not surprising that embryos from mothers lacking the Mei-41 checkpoint protein appear to develop normally during these cycles (Sibon *et al.* 1999).

Following NC 10, S-phase begins to increase in length to account for a reduction in replication origin firing and differential replication timing of specific regions within the DNA (Blumenthal *et al.* 1974; Shermoen *et al.* 2010). By NC 14 there is an overall increase in zygotic gene transcription coupled with the destruction of maternally loaded

mRNAs, including the mitotic activator Cdc25 (encoded by *string*), thus creating the first G2 phase (reviewed in O'Farrell *et al.* 1989). This switch from maternal to zygotic control of gene expression drives cellularization, the cytological hallmark of the midblastula transition (MBT), and all further morphological development of the embryo requires zygotic gene activity (Sibon *et al.* 1999; Shermoen *et al.* 2010; reviewed in Duronio 2012). Embryos from females lacking Mei-41 fail to slow nuclear cycles leading up to the MBT, resulting in abnormal nuclei, incompletely replicated DNA, and lack zygotic gene expression that ultimately results in a failure to cellularize and eventual embryonic degeneration (Sibon *et al.* 1999).

Meiotic Roles of Mei-41 in *Drosophila melanogaster*

Mei-41 was originally identified during an EMS screen for meiotic mutants in 1972 (the original allele is now known as *mei-41*^{1}). While *mei-41*^{1} mothers displayed a reduction in brood size, crossover patterning analysis was possible, suggesting the allele was hypomorphic. Progeny from *mei-41*^{1} mothers displayed a non-uniform decrease in CO coupled with a rise in NDJ events and a decrease in CO interference (Carpenter and Baker 1972; Baker *et al.* 1976). Crossover patterning experiments using null mutations of *mei-41* had, until recently (see Chapter 3), not been performed due to maternal-effect embryonic lethality, preventing progeny analysis.

During meiosis, crossover resolution is monitored by meiotic checkpoints to ensure proper DSB repair prior to division at meiosis I, and current literature looking at *mei-41* in a meiotic context primarily focuses on its role as a checkpoint protein. Roles for *mei-41* in checkpoint arrest were initially discovered while searching for mutations in pathways producing oocyte and egg morphology defects. Mislocalization of Gurken

(Grk), an oocyte-specific TGFa-like protein, results in dorsal-ventral and anterior-posterior axis defects such as ventralized eggshells, a phenotype associated with mutants unable to repair DSBs (reviewed in Schüpbach and Roth 1994). Identified female sterile mutants include *spnA* (RAD51), *spnB* (DMC1/RAD51-like), and *okr* (Rad54), and function in the meiotic recombinational repair of DSBs (Ghabrial *et al.* 1998; Staeva-Vieira *et al.* 2003). Mutations in these genes result in a Mei-41-dependent checkpoint arrest, delayed DSB repair, exhibit mislocalization of Gurken, and fail to establish dorsal-ventral polarity in the oocyte (Ghabrial and Schüpbach 1999; Jang *et al.* 2003). Similarly, in *S. cerevisiae*, the genes encoding the ATR and ATRIP homologs, *Mec1 and Ddc2*, respectively, are required for cellular arrest at prophase I due to unrepaired DNA breaks when RAD51 and DMC1 are absent (Bishop 1992; Refolio *et al.* 2011). Intriguingly, *tefu* mutants (DmATM) also exhibits GRK mislocalization due to unrepaired DSBs via the same Mei-41 dependent checkpoint (Joyce *et al.* 2011).

While Mei-41 has demonstrable checkpoint roles in *Drosophila*, it is also required for meiotic DSB repair (Joyce *et al.* 2011). Meiotic DSBs can be detected in the oocyte by the phosphorylated histone H2A variant, H2AV (γ-H2AV). Meiotic recombination completes in germarium region 3 (Figure 1.2), visualized by the absence of γ-H2AV (Mehrotra and McKim 2006). Germaria from homozygous null females show wild-type levels of γ-H2AV foci at the beginning of recombination in region 2A. However, unlike wild-type, foci persist at and beyond region 3 until the removal of H2AV at stage 5, implicating a role for Mei-41 in DSB repair in addition to its checkpoint function (Joyce *et al.* 2011). Interestingly, Mei-41 and Tefu are redundant for H2AV phosphorylation, as *mei-41; tefu* double mutants completely lack γ-H2AV foci (Joyce *et al.* 2011). Recent

studies utilizing AZ20, a selective ATR inhibitor, in adult male mice and cultured neonatal testes show a delay in RAD51 and DMC1 association at resected DSBs that is CHK1-dependent, suggesting loss of the ATR-CHK1 pathway inhibits meiotic strand exchange (Pacheco *et al.* 2017).

The mechanistic roles of Mei-41 at the *Drosophila* SC are not well understood. However, in mouse spermatocytes, where synapsis occurs after DSB initiation (reviewed in Dobson *et al.* 1994), ATR and its activator protein ATRIP co-localize to asynapsed chromosome axes and accumulate in regions where synapsis has been delayed, implicating ATR in monitoring chromosome asynapsis (Keegan *et al.* 1996; Refolio *et al.* 2011). Support for a role for ATR at the SC can also be found in *S. cerevisiae*. Mec1 (and Tel1/ATM) phosphorylation of the Hop1 SC axial element protein is required for interhomolog partner choice during meiotic recombination (Grushcow *et al.* 1999; Carballo *et al.* 2008).

Targeting Mei-41 in Meiotic Crossover Patterning

Due to the conserved mitotic role of ATR throughout many eukaryotes in responding to DSBs, we sought to gain a better understanding of how ATR functions specifically in the presence of meiotically-induced DSBs. Utilizing molecular genetics within the model organism *Drosophila melanogaster*, we were able to overcome the maternal embryonic lethality phenotype of *mei-41* null females. This allowed us to analyze CO patterning disruption and changes to CO patterning phenomena in a true *mei-41* null for the first time. We discovered that not all CO control phenomena are the result of a single patterning process, and that crossover patterning appears to be established in a stepwise manner, with the centromere effect first revoking CO-eligible

intermediates within the pericentric region prior to interference or assurance along the rest of the chromosome arm. This work opens new avenues of research regarding the establishment of the centromere effect as a critical component of proper crossover patterning during meiotic recombination.

CHAPTER 3

MEIOTIC CROSSOVER PATTERNING IN THE ABSENCE OF ATR: LOSS OF INTERFERENCE AND ASSURANCE BUT NOT THE CENTROMERE EFFECT[1]

Introduction

Meiotic crossovers are subject to numerous mechanisms of spatial control to ensure proper disjunction of homologous chromosomes and generation of genetic diversity. Sturtevant described the phenomenon of crossover interference, where the presence of one crossover reduces the probability of crossovers nearby (Sturtevant 1913, reviewed in Berchowitz and Copenhaver 2010). Mather pointed out that for small chromosomes "the chiasma frequency equals one, no matter what the size;" Owen referred to this as the "obligate chiasma" (Mather 1937; Owen 1949). The phenomenon in which every pair of homologous chromosomes has at least one crossover that generates a chiasma to promote disjunction is commonly called crossover assurance (reviewed in Wang *et al.* 2015). Together with crossover homeostasis, which buffers crossover formation from increases or decreases in potential crossover precursors (Martini *et al.* 2006), assurance and interference demarcate the minimum and maximum number of crossovers per meiosis. Modeling suggests that crossover assurance, interference, and homeostasis are the result of a single patterning process (Wang *et al.*

[1]This chapter is adapted from a manuscript currently in submission to *Genetics*.

2015). However, the mechanisms that achieve assurance, interference, and homeostasis remain obscure.

Less attention has been paid to the centromere effect, a spatial crossover patterning phenomenon first described by Beadle (Beadle 1932). Crossovers are excluded from the vicinity of centromeres in many organisms, presumably because very proximal crossovers can interfere with homolog disjunction (Koehler *et al.* 1996; Lamb *et al.* 1996). There are two components to the reduction in crossovers near the centromere. First, Muller and Painter reported that crossing over is absent or extremely rare within the “inert regions”, now known to comprise heterochromatic pericentromeric satellite sequence (Muller and Painter 1932). The second component, which we refer to as the centromere effect, is the phenomenon Beadle described: the reduction in crossing over within crossover-competent regions of the genome as a function of proximity to the centromere. Beadle noticed that when regions with high crossover density were moved closer to the centromere by chromosome rearrangement, crossover frequency decreased. The converse—increased crossover density when centromere-proximal regions are moved away from the centromere—was shown by Mather (Mather 1939).

The mechanisms underlying the centromere effect are also unknown. Meiotic recombination is initiated by formation of DNA double-strand breaks (DSBs). Each DSB can be repaired into a crossover or a non-crossover; the latter can be detected when they result in gene conversion, the unidirectional transfer of sequence from a donor (a homologous chromosome) to a recipient (the chromatid that received the DSB). In *Drosophila*, DSBs appear be to be excluded from the pericentric heterochromatin,

explaining the absence of crossovers on those regions (Mehrotra and McKim 2006). The centromere effect could in principle be explained by decreased DSB density in proximal regions. However, recent whole-genome sequencing reveals that the density of non-crossover gene conversion is relatively constant across the assembled genome on each arm (Comeron *et al.* 2012; Miller *et al.* 2016). This suggests that DSB density is also fairly constant across the chromosome arm and that the centromere effect is exerted by regulating the outcome of DSB repair (crossover or non-crossover) in a manner that is dependent on distance to the centromere.

Mutations in the Drosophila *mei-41* gene were first described by Baker and Carpenter (Baker and Carpenter 1972), who reported a polar reduction in crossovers, with a less severe effect on crossovers in proximal regions, and a possible decrease in interference. These observations suggest a potential role for Mei-41 in crossover patterning. Mei-41 is the Drosophila ortholog of ATR kinase, best known for regulating DNA damage-dependent cell cycle checkpoints (Hari et al. 1995). Consistent with this role, Mei-41 establishes a checkpoint that monitors progression of meiotic recombination (Ghabrial and Schüpbach 1999; Abdu et al. 2002). In addition, Mei-41 acts redundantly with ATM kinase to promote phosphorylation of histone H2AV at sites of meiotic DSBs (Joyce et al. 2011). However, it is unlikely that either of these functions explains the effects of crossover number or position noted by Baker and Carpenter. Understanding this role is further complicated by the finding that Mei-41 has an essential function in slowing the rapid nuclear cycles at the midblastula transition in embryonic development (Sibon et al. 1999). Females with null mutations in *mei-41* are sterile because this function is lost, and thus the alleles used in previous studies of

meiotic recombination are either hypomorphic or separation-of-function (Laurençon et al. 2003).

We sought to investigate the possible function for Mei-41 in crossover patterning by analyzing crossover distribution in *mei-41* null mutants. To overcome the requirement for maternal Mei-41, we used a transgene in which *mei-41* expression is under control of a promoter that turns on only after recombination has been completed, thereby generating a fertile *mei-41* "meiotic recombination null" mutant. We find that crossover and nondisjunction phenotypes are more severe in this mutant than in previously-reported hypomorphic mutants. We observe a polar effect on *2L* but not on the *X*; we suggest that this is due to retention of the centromere effect, which is weak on the *X*. However, interference and assurance are greatly decreased or lost. We propose that the centromere effect is established early in the meiotic recombination pathway and that Mei-41 has a recombination role after this establishment but before interference and assurance are achieved. Loss of Mei-41 leads to exit from the meiotic recombination pathway after establishment of the centromere effect and repair is then completed by alternative mechanisms that lack interference and assurance. These findings provide insight into establishment of crossover patterning.

Results

Post-germarium expression of mei-41 *rescues embryonic lethality and creates a meiotic recombination null*

Drosophila females homozygous for null mutations in *mei-41* produce no viable progeny due to a requirement for maternally-deposited Mei-41 at the midblastula transition (Sibon *et al.* 1999). *Blm* null mutants also exhibit maternal-effect embryonic

lethality (Mcvey *et al.* 2007). To study meiotic recombination in *Blm* null mutants, Kohl *et al.* expressed wild-type Blm under indirect control of the *alpha tubulin 67C* (*matα*) promoter via the Gal4-*UASp* system (Kohl *et al.* 2012). This promoter is specific to the female germline, with expression initiating in the early vitellarium (Sanghavi *et al.* 2013), by which time recombination should be compete. In support of this expectation, crossover and nondisjunction assays on the occasional surviving progeny of *Blm* mutant females give similar results to those from embryos rescued by expressing *UASp::Blm* with the *matα4::GAL4-VP16* driver in *Blm* null mothers (Mcvey *et al.* 2007; Kohl *et al.* 2012; Hatkevich *et al.* 2017).

We used the same system to overcome the maternal-effect inviability of embryos from *mei-41*^{29D} homozygous null females (see Materials and Methods). To quantify the extent of maternal *M*{*UASp::mei-41*} rescue, we compared hatch rates of embryos from wild-type, *mei-41*^{29D}, and *P*{*UASp::mei-41*} *mei-41*^{29D} with and without *P*{*matα4::GAL4-VP16*} (Table 3.1). Embryos from females homozygous for *mei-41*^{29D} with or without *M*{*UASp::mei-41*} but lacking *P*{*matα4::GAL4-VP16*} did not survive to hatching, whereas embryos from females with both components of the Gal4-*UASp* rescue system had a hatch rate of 52.8%. Most or all of the residual lethality is likely due to aneuploidy resulting from high nondisjunction in *mei-41* mutants (13.6% *X* nondisjunction among progeny surviving to adulthood; Tables 3.2a, b). Larvae that did hatch survived to adulthood, allowing for analysis of the crossover patterning landscape in a *mei-41* null mutant. For simplicity, flies carrying this transgene system are denoted below as *mei-41*^{29D} or *mei-41* null mutants.

Maternal Genotype	Hatched (%)	Total (*n*)
wild-type	73.1[a]	2035
mei-41^{29D}	0	527
P{*UASp::mei-41*} *mei-41*^{29D}	0	837
P{*UASp::mei-41*} *mei-41*^{29D}; *P*{*matα4::GAL4-VP16*} / +	52.8[b]	1187

Table 3.1. Hatch rates for embryos from *mei-41* mutants. Refer to Materials and Methods for details regarding hatch rates. [a] This number is lower than expected for wild-type. The cause of this is unknown. [b] The apparent lack of complete rescue may be the result of a high frequency of aneuploidy resulting from the absence of *mei-41* during meiotic recombination.

Crossover reduction in mei-41 *null mutants*

Drosophila mei-41 was initially characterized in 1972 as a meiotic mutant by Baker and Carpenter (Baker and Carpenter 1972). Hypomorphic *mei-41* alleles resulted in an overall 46% decrease in crossovers relative to wild-type controls, measured in five adjacent intervals spanning the entirety of *2L* and proximal *2R* (about 20% of the euchromatic genome). We measured crossovers in this same region in *mei-41* null mutant females and found a significantly more severe reduction of 67% ($p < 0.0001$; Figure 3.1A and 1B). Given the many functions of Mei-41 in mitotically proliferating cells, we wanted to determine whether the remaining crossovers were meiotic or possibly resulted from DNA damage within the pre-meiotic germline. As Mei-P22 is required to generate meiotic DSBs (Liu *et al.* 2002; Robert *et al.* 2016), any crossovers that are independent of Mei-P22 most likely result from damage occurring in pre-meiotic mitotic cell cycles or pre-meiotic S phase. Crossovers were completely abolished in *mei-41*^{29D}; *mei-P22*^{103} double mutants ($n = 1754$). One vial had two female progeny that were mutant for all markers on the *net–cn* chromosome except *pr*. These may have arisen from a double crossover in the adjacent *b–pr* and *pr–cn* regions, gene conversion

	Maternal Genotype	Normal Progeny	Nondisjunction Progeny		*X* NDJ (%)	
			XO ♂♂	*XXY* ♀♀		
1	*mei-41*^{1}	815	24	15	8.7	± 2.7
2	*mei-41*^{29D}	3791	144	155	13.6	± 1.5
3	*mei-9*^{a}	287	25	27	26.5	± 6.7
4	*mei-9*^{a} *mei-41*^{29D}	499	27	20	15.9	± 4.4
5	*mei-9*^{a} *mei-41*^{29D} / *mei-9*^{a}	354	31	37	27.7	± 6.1
6	*mei-9*^{a} *mei-41*^{29D} / *mei-9*^{a}	521	36	52	25.3	± 4.9

Table 3.2a. *X* nondisjunction. *X* chromosome nondisjunction (NDJ) was scored as described in Materials and Methods. Genotypes 1-4 were homozygous for the indicated mutant alleles. All *mei-41*^{29D} experiments had the *M*{*UASp::mei-41*} and *P*{*matα::GAL4*} transgenes described in the text. Genotypes 5 and 6 were made by crossing each of the two stocks that were used to generate *mei-9 mei-41* double mutants to *mei-9*^{a} single mutants to test for the presence of *mei-9*^{a} in the stock. The males used to generate genotype 5 were *y M*{*UASp::mei-41*} *mei-9*^{a} *mei-41*^{29D} on the *X* chromosome. The males used to generate genotype 6 were *y mei-9*^{a} *mei-41*^{29D} on the *X*. Statistical analyses are in Table S5b, below. *p* values are not corrected for multiple comparisons, but such corrections would not change any conclusions.

Genotypes	*p*	Interpretation
1 *vs.* 2	0.0020	NDJ is significantly higher in *mei-41*^{29D} than in *mei-41*^{1}, supporting the conclusion that *mei-41*^{1} is a hypomorphic allele.
2 *vs.* 3	0.0002	NDJ is significantly higher in *mei-41*^{29D} than in *mei-9*^{a}. (Genotypes 5 and 6 were homozygous for *mei-9*^{a} and heterozygous for *mei-41*^{29D}
2 *vs.* 5	<0.0001	
2 *vs.* 6	<0.0001	
2 *vs.* 4	0.3420	NDJ in *mei-9*^{a} *mei-41*^{29D} double mutants is not significantly different from NDJ in *mei-41*^{29D} single mutants.
3 *vs.* 5	0.8033	NDJ is not significantly different between the three *mei-9* single mutants, confirming the presence of the *mei-9*^{a} mutation in the stocks used to generate *mei-9*^{a} *mei-41*^{29D} double mutants (also confirmed by allele-specific PCR).
3 *vs.* 6	0.7516	
5 *vs.* 6	0.5324	

Table 3.2b. Statistical comparisons of *X* nondisjunction. Methods of Zeng *et al.* (2010) was used to calculate *X* nondisjunction (NDJ) with 95% confidence intervals and to calculate *p* values based *Z* tests. *p* values are not corrected for multiple comparisons, but such corrections would not change any conclusions.

of the *pr* mutation, or reversion of this mutation (an insertion of a *412* transposable element). Since these were in the same vial they likely represent a single pre-meiotic event. We conclude that the vast majority of crossovers observed in the *mei-41* null mutant females are meiotic in origin.

Baker and Carpenter described crossover reduction in *mei-41* hypomorphic mutants as polar, with a more severe decrease in medial and distal regions of the chromosome than in proximal regions (Baker and Carpenter 1972). This is also true in our null mutant: Although crossovers are significantly reduced in every interval, the average reduction in the three distal intervals is 75%, while in the two proximal intervals the decrease averages only 16% (Figure 3.1B). We also assayed crossing over across the entire *X* chromosome. Crossovers were reduced by an average of 57% on this chromosome; notably, the decrease was uniform across the entire chromosome, with no apparent polar effect (Figure 3.1C and 3.1D).

One hypothesis to explain the polar effect on recombination on *2L* is that there are region-specific requirements for Mei-41, with the protein being less important in proximal *2L*. We tested this hypothesis by assessing the dependence of crossovers on Mei-9, the catalytic subunit of the putative meiotic resolvase (Sekelsky *et al.* 1995). Meiotic crossovers are reduced by about 90% in *mei-9* mutants, suggesting that most or all crossovers generated in wild-type flies require Mei-9 (Figure 3.1E) (Baker and Carpenter 1972; Sekelsky *et al.* 1995). However, in many mutants that affect meiotic recombination, including *Blm*, *mei-218*, and *rec*, crossovers are independent of Mei-9 (Sekelsky *et al.* 1995; Blanton *et al.* 2005; Hatkevich *et al.* 2017). Our interpretation is that when the meiotic crossover pathway is blocked because of loss of a critical

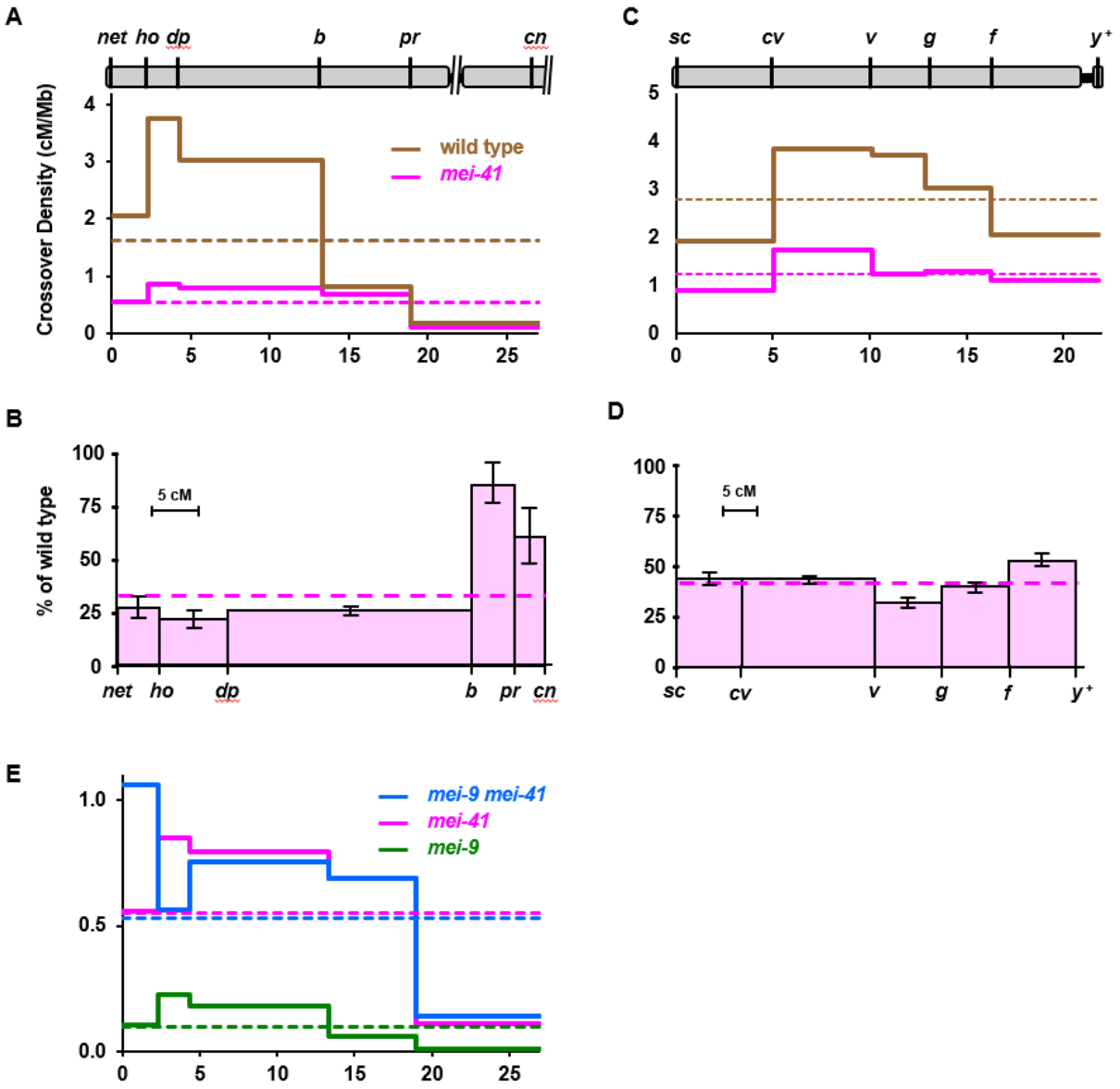

Figure 3.1. Reduction of crossing over in *mei-41* null mutants. (A) and (C) Crossover distribution on *2L* (A) and *X* (C) in *mei-41*^{29D} mutants compared to wild-type. Marker location indicated at top based on genome assembly position (Mb), excluding the centromere and unassembled pericentromeric satellite sequences (*ho* = *dpp*$^{d\text{-}ho}$). Crossover density (solid lines) was determined for wild-type and *mei-41* null mutant females. Dotted lines show mean crossover density across the entire region. (B) and (D) Crossing over on 2L (B) and X (D) in *mei-41*^{29D} mutants as a percentage of wild-type. The X axis is scaled to genetic distance (cM) in wild-type females. Bars are 95% confidence intervals. (E) Crossover density in *mei-9* and *mei-41* single and double mutants. Note scale difference compared to (A). Wild-type *2L*: *n* = 4222 progeny, 1943 crossovers; mei-41 *2L*: *n* = 7801 progeny, 1175 crossovers. Wild-type *X*: *n* = 2179 progeny, 1367 crossovers; mei-41 *X*: *n* = 5174 progeny, 1396 crossovers; *mei-9*: *n* = 2433 progeny, 67 crossovers; *mei-9 mei-41*: *n* = 1059 progeny, 165 crossovers. Wild-type and *mei-9* single mutant data are from Hatkevich *et al.* (2017), used with permission. Full datasets are in Tables 3.3-3.4.

component, repair is completed by alternative pathways that are independent of Mei-9 and other downstream meiotic recombination proteins. If Mei-41 is less important in proximal *2L*, then crossovers in these regions may remain dependent on Mei-9. We scored crossovers along *2L* in *mei-9^{a} mei-41^{29D}* double mutants (Figure 3.1E; we did not score the *X* chromosome because of the difficulty in recombining the *mei-9* and *mei-41* mutations and the *UASp::mei-41* transgene onto the multiple-marked chromosome, and the requirement for Mei-41 appeared to be similar across the *X*). The total genetic map length was similar between *mei-9 mei-41* double mutants and *mei-41* single mutants (15.58 cM *vs* 15.06 cM; $p = 0.6679$ by χ^2 test comparing total crossovers and number of progeny scored) but significantly greater than that of *mei-9* mutants (2.8 cM; $p < 0.0001$). There was no apparent difference in requirement for Mei-9 between the proximal and distal intervals. We conclude that all crossovers generated in *mei-41* mutants are independent of *mei-9*, regardless of chromosomal location. This suggests that loss of Mei-41 disrupts progression through the meiotic crossover pathway at all sites along the chromosome.

The apparent polar effect on crossing over in **mei-41** *mutants can be explained by retention of the centromere effect*

Compared to wild-type crossing over, the effects of loss of Mei-41 on meiotic crossing over is puzzling, as there seem to be substantially stronger effects in some regions of the genome than others, yet all crossovers in the mutant are independent of Mei-9. The conclusion that there is a polar effect on crossing over is based on comparing crossover frequencies in the mutant to those in wild-type females. Insight can also be gleaned by analyzing crossover distribution in the mutant in isolation. For example, Hatkevich *et al.* noted an apparently flat distribution of crossover in mutants

lacking the Blm helicase. Their interpretation was that all crossover patterning is lost in *Blm* mutants, resulting in a distribution that reflects the DSB distribution (Hatkevich *et al.* 2017).

Crossover distribution in *mei-41* mutants does not mimic that of *Blm* mutants, at least in proximal *2L*, suggesting that crossover patterning is not entirely lost in *mei-41* mutants. In wild-type flies, crossover density is substantially lower in the *pr–cn* interval than in any of the other nine intervals that we assayed (0.11 ±0.03 cM/Mb, versus 0.56 ±0.09 in the next lowest interval, *net–ho*). The *pr–cn* interval is noteworthy because it spans the centromere, so recombination is strongly influenced by the centromere effect. To determine whether this phenomenon is affected by loss of Mei-41, we calculated *CE* as a measure of the centromere effect (see Materials and Methods; Hatkevich *et al.* 2017). In wild-type females, if crossover density in this interval were equal to the mean density across the entire region assayed, 643 crossovers would be expected; only 73 were observed ($p < 0.0001$), giving a *CE* value of 0.89. In *mei-41*^{29D} mutants, 390 were expected but only 82 were observed ($p < 0.0001$), yielding a *CE* value of 0.79. This high value of *CE* indicates that most or all of the centromere effect is intact in *mei-41*^{29D} mutants, although the significant difference between *mei-41*^{29D} and wild-type females ($p = 0.0004$) suggests that there may be mild amelioration in *mei-41* mutants.

The decrease in crossing over on the *X* chromosome does not appear to be polar (Figure 3.1C and Figure 3.1D). The pericentric heterochromatin of the *X* chromosome spans about 19 Mb, compared to about 5 Mb on *2L* and 7 Mb on *2R*. This results in a much weaker centromere effect on the *X* chromosome (0.29 in the *f–y*$^{+}$ interval wild-type flies) (Yamamoto 1978). The lack of a polar decrease in crossing over on the *X* in

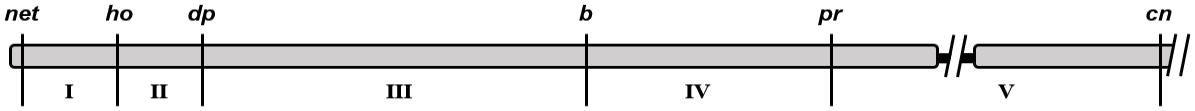

Progeny		Maternal Genotype					
		WT1	***WT2***	***WT1+2***	***mei-41***	***mei-9***	***mei-9 mei-41***
Parental		1053	1223	2376	6667	2366	904
SCO	I	70	106	176	87	6	22
	II	127	163	290	119	11	5
	III	497	602	1099	530	40	69
	IV	89	65	154	286	8	39
	V	23	16	39	71	2	11
DCO	I / II	1	0	1	3	0	3
	I / III	4	7	11	6	0	0
	I / IV	7	3	10	4	0	0
	I / V	0	2	2	1	0	0
	II / III	1	5	6	7	0	2
	II / IV	5	2	7	2	0	1
	II / V	8	5	13	2	0	0
	III / IV	10	9	19	8	0	0
	III / V	7	10	17	6	0	1
	IV / V	1	1	2	2	0	1
TCO		0	0	0	0	0	1
n		1903	2319	4222	7801	2433	1059

Table 3.3. Meiotic crossovers on chromosome *2L*. Each row lists the number of total progeny from parental or single (SCO), double (DCO), or triple (TCO) crossover classes for wild-type (*WT*) and *mei-41* null mutants. Intervals I to V correspond to schematic above. Wild-type data were collected by different individuals in different years (see Material and Methods); the individual datasets and the summed set, which was used in all analyses, are given. The TCO in *mei-9 mei-41* was intervals I/II/IV. Wild-type data are from Hatkevich *et al.* (2017), used with permission (RightsLink license 4217090536151, 27 Oct 2017).

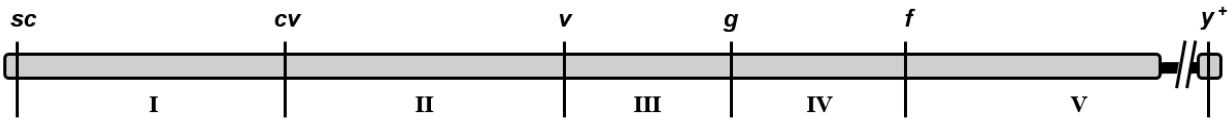

Progeny		Maternal Genotype	
		WT	***mei-41***
Parental		1015	3929
SCO	I	148	178
	II	333	370
	III	162	121
	IV	155	174
	V	166	258
DCO	I–II	5	15
	I–III	18	14
	I–IV	20	8
	I–V	29	10
	II–III	25	20
	II–IV	44	22
	II–V	26	24
	III–IV	6	7
	III–V	14	6
	IV-V	10	11
TCO		3	7
n		2179	5174

Table 3.4. Meiotic crossovers on chromosome *X*. Each row lists the number of progeny from parental or single (SCO), double (DCO), or triple (TCO) crossover classes for wild-type (*WT*) and *mei–41* null mutants. Intervals I to V correspond to schematic above. The TCOs in wild/type flies were one each in intervals (II/III/V), (II/IV/V), and (III/IV/V). TCOs in *mei-41* were one each in intervals (I/II/III), (I/II/IV), (I/II/V), (I/III/V), and (II/IV/V) and two each in intervals (II/III/IV) and (II/IV/V). Wild-type data are from Hatkevich *et al.* (2017), used with permission (RightsLink license 4217090536151, 27 Oct 2017).

mei-41 mutants may be because the entire region being analyzed is, with respect to distance from the centromere, equivalent to the distal half of *2L*.

The small chromosome *4* of *Drosophila melanogaster* never has meiotic crossovers in wild-type females, but does have crossovers in *Blm* mutants (Hatkevich *et al.* 2017, reviewed in Hartmann and Sekelsky 2017). Hatkevich *et al.* argued that the absence of crossovers on *4* is due in large part to the centromere effect (about 4 Mb of heterochromatic satellite sequence between the centromere and the gene-containing region), and that it is loss of the centromere effect that permits crossing over on *4* in *Blm* mutants. We measured crossing over on *4* in *mei-41* mutants. We recovered no crossovers between *ci* and *sv* (n = 5555; $p < 0.0001$ compared to *Blm*), consistent with our interpretation that the centromere effect is not lost in *mei-41* mutants.

Loss of crossover interference and crossover assurance in mei-41 *null mutants*

Given the apparent retention of the centromere effect on crossing over, we asked whether the crossover patterning phenomena interference and assurance are impacted by loss of Mei-41. We calculated interference (I) using the method of Stevens (Stevens 1936). Stevens defined I as 1-(O/E), where O is the number of double crossovers observed and E is the number of double crossover expected if the two intervals are independent of one another (see Materials and Methods). Thus, I = 1 indicates complete positive interference (no double crossovers observed) and I = 0 indicates no interference (the two intervals are independent of one another).

Values for O, E, and I are given in Figure 3.2A and 3.2B. On *2L*, the only pairs of adjacent intervals that have enough double crossovers to analyze interference are II-III

(*ho–dp* and *dp–b*) and III-IV (*dp–b* and *b–pr*). In wild-type females, *I* was 0.93±0.05 between intervals II and III ($p < 0.0001$) and 0.64±0.15 between intervals III and IV ($p = 0.0001$). In *mei-41* mutants, we did not detect significant interference in the first pair of intervals ($I = 0.26±0.52$, $p = 0.25$; $p < 0.0001$), but interference appeared to be intact between the second pair of intervals ($p = 0.9922$ compared to wild type). The *dp* to *b* interval is typically not used for measuring interference because of its large size (>27 cM). Therefore, we reexamined interference within this region by subdividing it with another marker, $wg^{Sp\text{-}1}$. Again, interference was strong in wild-type females but absent from *mei-41* mutants (Figure 3.2A, lower section). Using the same analysis of interference across the *X* chromosome, we found significant positive interference between every pair of adjacent intervals in wild-type females, but no detectable interference in *mei-41* mutants (Figure 3.2B).

We used one additional method to assess the distribution of crossovers relative to one another. In many species, crossovers are distributed among bivalents such that the probability that any pair of homologous chromosomes does not receive a crossover is significantly lower than expected by chance, a phenomenon known as crossover assurance. It has been proposed that if there are sufficient well-spaced crossover-eligible intermediates, then coupling interference with a mechanism to achieve a specific number of crossovers per meiosis (within a narrow range) will produce crossover assurance (Zhang *et al.* 2014; Wang *et al.* 2015). In this model, assurance is merely an outcome of interference.

Extrapolating from our measurements of crossovers on *X* and *2L*, we estimate about two crossovers per meiosis in *mei-41* mutants. True assurance requires a

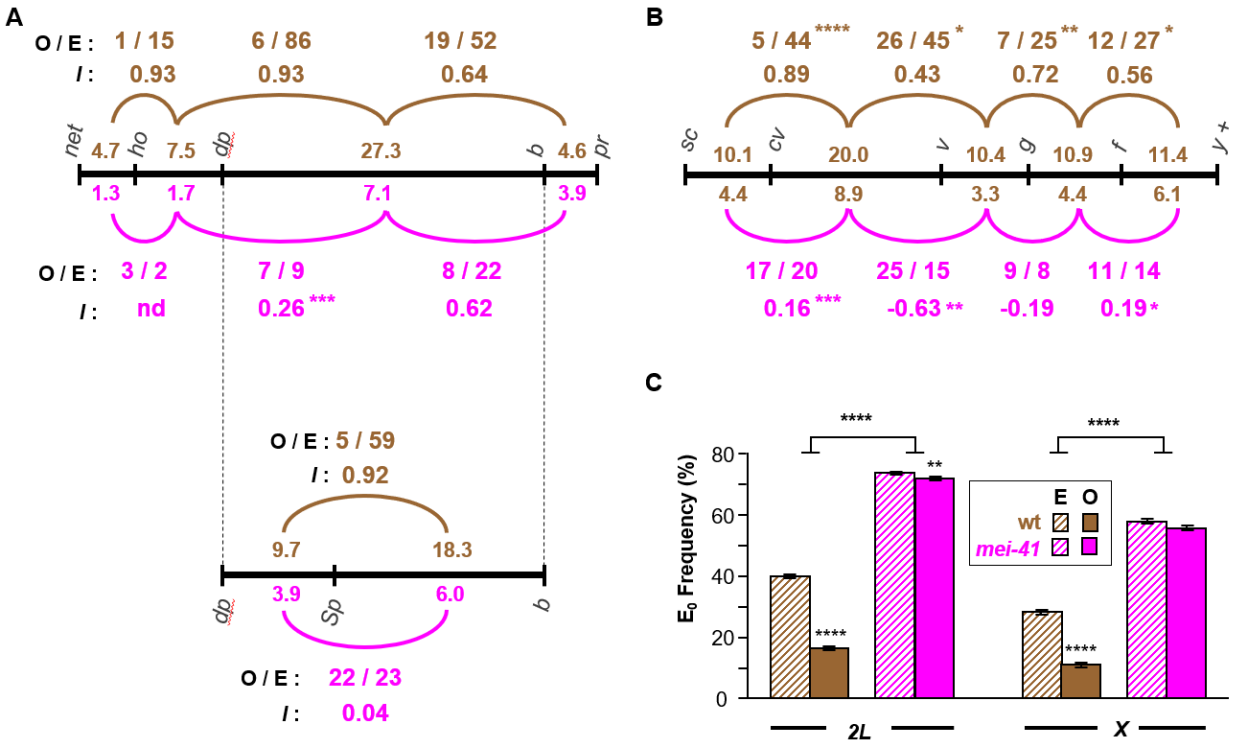

Figure 3.2. Interference and assurance in *mei-41* null mutants. (A) Interference on *2L*. Black line represents genetic map of markers used, with size of each interval (in cM) listed above the line for wild-type females and below the line for *mei-41* mutants. The *pr–cn* interval was omitted because it spans the centromere and because of low numbers of double crossovers in between this and the adjacent interval. Arcs represent pairs of adjacent intervals in which interference was tested. Above (for wild-type, brown) or below (*mei-41*, pink) each arc is listed the number of observed double crossovers (O) and the number expected (E) if the two intervals are independent (no interference). Asterisks indicate *p* values for the difference between O and E. Stevens' interference (*I*), which equals 1-(O/E), is also given. Asterisks on *I* values indicate *p* values for χ2 analysis of O and E for wild-type and mutant (see Materials and Methods). In a separate experiment, the large *dp–b* interval was further divided by the addition of *Sp* ($wg^{Sp\text{-}1}$). (B) Similar analysis of interference on the *X* chromosome. The *f-y+* region spans the centromere, but since the marker on the right arm (*y+*) is hemizygous (*i.e.*, a duplication of the tip of *XL* on onto *XR* on one homolog), all crossovers must be to the left of the centromere. (C) Crossover assurance assessed by comparing frequencies of E_0 bivalents. Expected E_0 frequency is based on Poisson distribution from the average number of crossovers per meiosis; observed frequencies were calculated using the method of Weinstein (Weinstein 1936). Statistical significance between expected and observed E_0 frequencies determined via χ2 tests. Bars show 95% confidence intervals. Sample sizes for *2L* and *X* are given in Figure 3.1. For the *dp-Sp-b* experiment, *n* = 3325 flies, 928 crossovers for wild-type; *n* = 9740 flies, 972 crossovers. * $p < 0.05$, ** $p < 0.01$, *** $p < 0.001$, **** $p < 0.0001$.

Progeny Class	Progeny Genotype	Maternal Genotype	
		wild-type	***mei-41^{29D}***
Parental	+ + +	1510	5200
	dp Sp b	1897	3686
Single Crossover	+ *Sp b*	172	195
	dp + +	144	164
	+ + *b*	344	272
	dp Sp +	258	297
Double Crossover	+ *Sp* +	4	17
	dp + *b*	1	5
Total *n*		3330	9836

Table 3.5. Progeny counts from *dp–Sp–b* interference experiment. Each row lists the number of progeny from parental and single (SCO), or double (DCO) classes for wild-type (*WT*) and *mei-41* null mutants.

minimum of three or five crossovers (one per major chromosome or arm, excluding *4*); however, assurance among the residual crossovers could manifest as the two crossovers being on different chromosomes (or chromosome arms) more often than expected by chance. We compared the expected and observed frequency of meioses in which there were no crossovers (E_0, for zero-exchange bivalent, frequency) on *X* or on *2L*. For expected E_0 frequency we used the Poisson distribution expectation based on the average number of crossovers per meiosis. We used the method of Weinstein to transform counts of progeny that inherited parental, single crossover, double crossover, etc., chromatids to bivalent exchange classes (Weinstein 1936, see Materials and Methods). In wild-type flies, the expected E_0 frequency for the *X* chromosome is 0.285, but the observed frequency was 0.112 (Figure 3.2C). This demonstrates crossover assurance that is significant ($p < 0.0001$) but incomplete (11% of meioses have no

crossovers between the *X* chromosomes), as has been observed in previous studies (e.g., Weinstein 1936; Koehler *et al.* 1996). In *mei-41* mutants, reduced crossing over results in a higher expected E_0 frequency (0.582), but unlike the case in wild-type flies, the observed frequency (0.572) was not significantly different ($p = 0.3008$). Similar results were obtained with the *2L* data (Figure 3.2C). For *2L*, the difference between observed and expected in *mei-41* mutants was significant ($p = 0.0046$), but given the small magnitude of the difference (0.740 expected, 0.720 observed), this may not be biologically meaningful.

Together, our data indicate that interference and assurance are significantly decreased or lost in *mei-41* mutants, though it is possible that crossovers in proximal *2L* retain interference.

Discussion

We have demonstrated that the Gal4-*UASp* rescue successfully overcomes maternal-effect embryonic lethality of *mei-41* mutants, allowing us to perform meiotic crossover patterning analysis in *mei-41* null mutants. The crossover reduction in null mutants is more severe than that of the previously reported for hypomorphic mutants, but the non-uniform effect on crossing over on chromosome *2* is still present (Figure 3.1B) (Baker and Carpenter 1972).

We considered the hypothesis that the polar effect stems from differential requirement for Mei-41 in proximal and distal regions of the chromosome. However, in *mei-41* mutants, crossovers in all regions are independent of the presumptive resolvase Mei-9 (Figure 3.1C). Our interpretation is that this reveals an essential role for Mei-41 in carrying out meiotic recombination throughout the genome. In the absence of Mei-41

the meiotic pathway is disrupted and repair is completed by alternative pathways that neither require functions specific to the meiotic pathway nor result in properties normally associated with meiotic recombination, such as crossover patterning.

Since the apparent polar effect is observed on *2* but not on the *X*, we hypothesized that the centromere effect is retained in *mei-41* mutants. We calculated *CE*, a measure of how much crossover density in an interval deviates from the mean crossover density, to compare the centromere effect between wild-type females and *mei-41* mutants (Hatkevich *et al.* 2017). Although every interval deviates significantly from the mean in wild-type flies, that the very strong deviation in the *pr–cn* region (*CE* = 0.89) is probably due primarily to the suppression of crossovers associated with proximity to the centromere. Direct confirmation of the presence of a centromere effect requires moving the sequences to be analyzed away from the centromere through chromosome rearrangement, a difficult experiment because of the need to have structural homozygosity combined with heterozygosity for markers. Nonetheless, our data suggest that a strong centromere effect is retained in the absence of Mei-41.

In contrast to the absence of a strong impact on the centromere effect, our analysis suggests that interference and assurance are significantly disrupted when Mei-41 is absent. It is notable that the only pair of intervals in which we detect significant interference includes the *b–pr* interval (IV), which is the closest interval to the centromere that we could analyze (in the two most proximal intervals, IV and V*,* there were too few double crossovers expected [three] and observed [two]). This could indicate that Mei-41 does have different functions in proximal regions than in other parts of the genome. However, given that there appears to be no interference within the

adjacent interval III, the presence of interference between III and IV would require that crossover-eligible intermediates in III be subject to interference exerted by crossover designations in IV, while at the same time any crossovers designated within III not signal interference themselves. This seems unlikely, and perhaps indicates that there is some other effect or some idiosyncrasy associated with this particular interval.

Another argument that interference is reduced or absent in *mei-41* mutants is that the strength of interference is inversely proportional to genetic size of interval in which it is measured. Therefore, since genetic intervals become shorter in *mei-41* mutants, interference might be expected to become stronger. This expectation would not hold for recombination proteins required to generate crossovers after interference has occurred, such as the proteins that resolvase crossover-designated intermediates into crossovers (the “crossover maturation” step in the models of Zhang *et al.* 2014). Mei-9 and associated proteins are thought to be required for resolution (Baker and Carpenter 1972; Sekelsky *et al.* 1995; Yıldız *et al.* 2002). It is not meaningful to discuss interference in *mei-9* mutants, since the number of crossovers per meiosis is well below one (0.06), but the uniform decrease in crossovers across *2L* led Baker and Carpenter to conclude that Mei-41 acts earlier in crossover generation than Mei-9 (Baker and Carpenter 1972).

We believe the most parsimonious interpretation of our data is that loss of Mei-41 has little or no impact on the centromere effect but reduces or eliminates interference and assurance. We propose that crossover patterning in *Drosophila* occurs in a stepwise manner (Figure 3.3). Analysis of non-crossover gene conversion events mapped through whole-genome sequencing suggests that DSBs are, at a large scale,

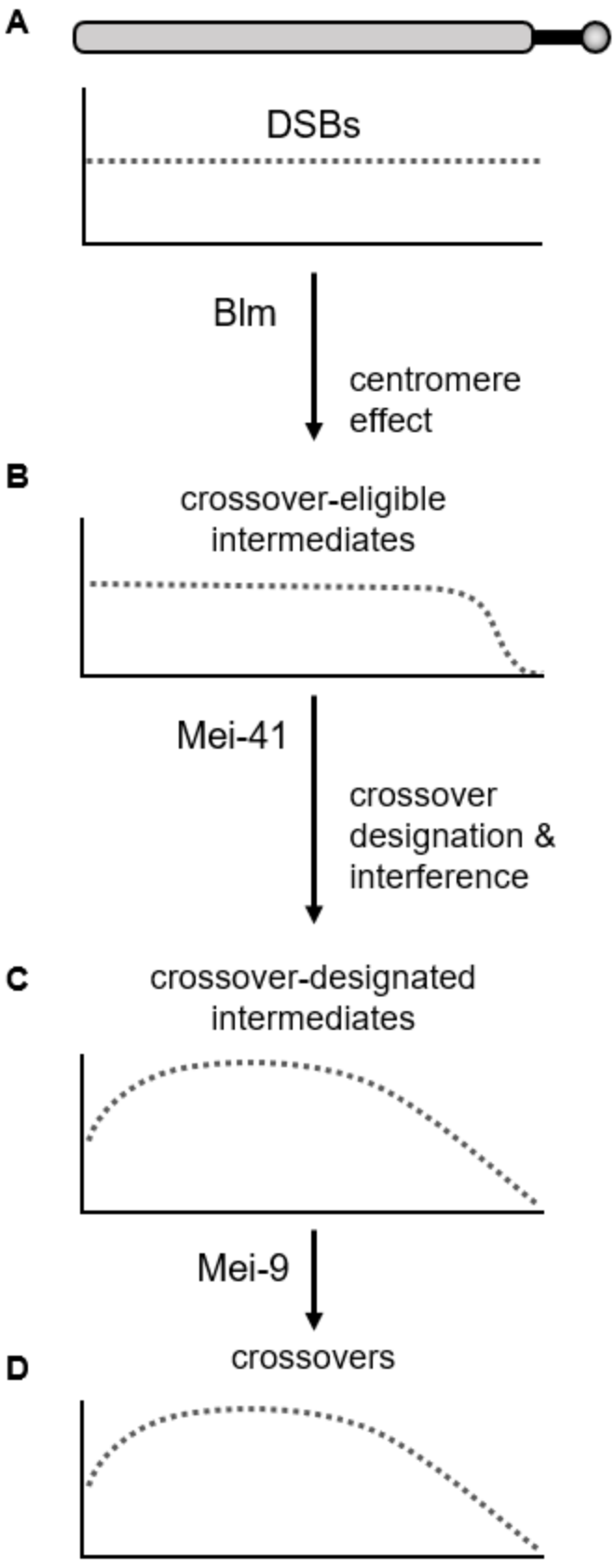

Figure 3.3. Model for progressive enforcement of crossover patterning. The drawing at the top represents a chromosome arm. Solid black line is pericentric satellite DNA, circle is centromere. (A) Based on whole-genome sequencing, the initial DSB distribution (dotted line) is flat at large scales (Comeron *et al.* 2012; Miller *et al.* 2016; Hatkevich *et al.* 2017); DSBs are excluded from the heterochromatic satellite DNA (Mehrotra and McKim 2006). The centromere effect revokes the eligibility of intermediates near the centromere from becoming crossovers. (B) This results in a distribution of crossover-eligible intermediates that is flat across much of the arm, then tailed as the centromere is approached. The shape of the tailing is unknown; a sigmoidal drop is shown here for illustrative purposes. Later, some intermediates are designated to become crossovers, and the resultant interference discourages other intermediates over large distances from achieving crossover designation. The resultant distribution of crossover-designated intermediates (C) and crossovers (D) is approximately skew normal, with the degree of skew being proportional to the length of satellite sequence that separates DSB-competent regions from the centromere. Blm, Mei-41, and Mei-9 are essential at different times in the crossover pathway, so crossovers generated in mutants that lack these proteins are made outside the normal meiotic pathway, and are therefore Mei-9-independent, and are either unpatterned (*Blm* mutants, distribution similar to panel A), are partially patterned (*mei-41* mutant, resembles panel B), or are fully patterned (*mei-9* mutant, resembles panels C and D).

spread evenly throughout the assembled genome (Comeron *et al.* 2012; Miller *et al.* 2016; Hatkevich *et al.* 2017). The centromere effect is applied early by making some intermediates ineligible to enter the crossover pathway, with the probability of being affected in this way being related to distance to the centromere (Figure 3.3B). Subsequently, when any remaining crossover-eligible intermediate becomes crossover-designated, interference precludes nearby intermediates from also adopting this fate (Figure 3.3C).

Given a uniform distribution of DSBs and the fact that each of the chromosome arms in *Drosophila* has about 1.0-1.3 crossovers per meiosis, interference alone will produce a crossover density that resembles a normal distribution (e.g., the simulations of Zhang *et al.* 2014). The combination of a strong centromere effect and interference will yield a crossover density map that approximates a skew normal distribution (Figure 3.3D). Crossover distribution maps in *Drosophila* do resemble skew normal distributions, with much more skew on the major autosome arms than on the *X*, which also lacks a strong centromere effect (see Figure S2 in Comeron *et al.* 2012).

Blm helicase has been proposed to have an essential function early in the meiotic recombination pathway (reviewed in Hatkevich and Sekelsky 2017). Loss of Blm results in an early exit from the meiotic pathway and completion of repair by alternative mechanisms. Since these alternative mechanisms do not involve patterning, the probability of becoming a crossover is the same for each intermediate, resulting in crossovers being evenly distributed across each chromosome arm. We propose that Mei-41 has some critical function after the centromere effect has been at least partially established. Loss of Mei-41 leads to exit from the meiotic pathway at this point. As with

Blm mutants, every remaining intermediate has the same probability of becoming a crossover, so the crossover distribution in *mei-41* mutants is similar to the that in Figure 3.3B. Mei-9 is required only for maturation of crossover-designated intermediates into crossovers. Since this occurs after crossover designation, residual crossovers in a *mei-9* mutant are patterned like crossovers in wild-type flies, but there are far fewer crossovers because most intermediates that had been designated to become crossovers are instead processed into non-crossover products.

In many model organisms, a subset of crossovers do not participate in interference and are generated by different resolvases than those that generate interfering crossovers (reviewed in Kohl and Sekelsky 2013). These “Class II” crossovers are sometimes defined as lacking interference or being unpatterned. In the model discussed above, this distinction is not always appropriate, at least in mutant situations. Rather, crossovers generated outside of the primary pathway may be unpatterned (as in *Blm* mutants), partially patterned (as in *mei-41* mutants), or patterned (as in *mei-9* mutants). The only features that these crossovers have in common is that they are generated outside of the normal meiotic crossover pathway, presumably through general DSB repair pathways that act to ensure there are no unrepaired DNA structures persisting until the meiotic divisions begin.

Our data provide little insight into the molecular function of Mei-41 in the meiotic DSB repair pathway. In mitotic DSB repair, *mei-41* mutants have no observable defects in the early steps of homologous repair of DSBs (*e.g.*, resection, strand invasion, and repair synthesis), but Mei-41 appears to be required for the annealing or ligation steps of synthesis-dependent strand annealing (SDSA; Larocque *et al.* 2007). Holsclaw and

Sekelsky hypothesized that Mei-41 activates Marcal1, which then catalyzes annealing of complementary sequences (Holsclaw and Sekelsky 2017). SDSA promotes formation of non-crossover products, in contrast to the apparent role for Mei-41 in promoting crossovers during meiotic recombination. Nonetheless, Mei-41 might have a similar function in mitotic and meiotic DSB repair if in the latter it activates a protein that catalyzes the annealing required for 2nd-end capture, a process that might occur after an early requirement for Blm helicase but prior to crossover designation (*e.g.*, models in Crown 2014). Future studies to elucidate the role for Mei-41 might provide additional insights into meiotic crossover pathways and patterning.

Materials and Methods

Drosophila stocks

Flies were maintained at 25˚C on standard medium. To overcome the maternal-effect embryonic lethality of *mei-41*^{29D} null mutation (Sibon *et al.* 1999; Laurençon *et al.* 2003), wild-type genomic *mei-41* was cloned into the *P*{*attB*, *UASp::*, *w*$^{+m}$} vector (courtesy of Steve Rogers) via In-Fusion HD (Takara Bio USA, Inc., Mountain View, CA) and transformed into XL10-Gold ultracompetent cells (Agilent Technologies, Inc., Santa Clara, CA). This construct was injected via phiC31 integrase-mediated transgenesis into the *X* chromosome landing site *M*{*3xP3-RFP.attP'*}ZH-2A (BestGene Inc., Chino Hills, CA). The resulting integrants, abbreviated herein as *M*{*UASp::mei-41*}, were crossed into a *P*{*matα4::GAL4-VP16*} background. All *mei-41* null assays used the genotype:

$$\frac{w\ mei\text{-}41^{29D}}{y\ M\{UASp{::}mei\text{-}41\}\ w\ mei\text{-}41^{29D}};\ \frac{P\{mat\alpha :: GAL4\text{-}VP16\}}{+}$$

The *mei-41 mei-P22* double mutant genotype was as above except the *3rd* chromosomes were *mei-P22^{103} st* / *mei-P22^{103} Blm^{D2} Sb P*{*matα4::GAL4-VP16*}. The *mei-9 mei-41* double mutant genotype was as above except the *X* chromosomes were *y mei-9^{a} mei-41^{29D}* / *y M*{*UASp::mei-41*} *w mei-9^{a} mei-41^{29D}*. The presence of the *mei-9^{a}* mutation was confirmed by allele-specific PCR and by genetic tests (see Table 3.2a).

Double mutant stock creation used the above transgenic rescue in conjunction with appropriate null alleles. The *mei-41 mei-P22* double mutant genotype was *y w mei-41^{29D}* / *y M*{*UASp::mei-41*} *w mei-41^{29D}*; *mei-P22^{103} st* / *mei-P22^{103} Blm^{D2} Sb P*{*matα4::GAL4-VP16*}. The *mei-9 mei-41* double mutant genotype was *y mei-9^{a} mei-41^{29D}* / *y M*{*UASp::mei-41*} *w mei-9^{a} mei-41^{29D}*; *P*{*matα4::GAL4-VP16*} / +.

Hatch rates

To test *M*{*UASp::mei-41*} rescue efficiency, 60 virgin females of appropriate genotypes were crossed to 20 isogenized Oregon-Rm males (courtesy of Scott Hawley). Adults were mated in grape-juice agar cages containing yeast paste for two days prior to collection. Embryos were collected on grape-juice agar plates for five hours and scored for hatching 48 hours later.

Crossover assays and analyses

Meiotic crossovers on *2L* were quantified by crossing *net dpp^{d-ho} dp b pr cn* /+ virgin females of the appropriate mutant background to *net dpp^{d-ho} dp b pr cn* males. All six markers were scored in progeny from each genotype, with the of exception *mei-41*; *mei-P22*. In that case, 731 *XX* females were scored for all six markers and an additional 1023 *XXY* females and *XY* males were scored for *net–b*; eye color markers *pr* and *cn* were excluded because of the presence of a *w* mutation in the mothers. These data

were pooled for a final *n* of 1754 progeny scored. Meiotic crossovers on *X* were quantified by crossing *y sc cv v g f · y*$^{+}$ virgin females of the appropriate background to *y sc cv v g f* male. "*· y*$^{+}$" is *Dp(1;1)sc*^{V1}, a duplication of the left end of the *X*, carrying *y*+, onto *XR*. All six markers were scored in all progeny. To measure chromosome *4* crossovers, the *mei-41* rescue genotype given above was made heterozygous for *PBac*{*y*$^{+}$ *w*$^{+m}$}(101F) and *sv*$^{spa\text{-}pol}$, which are near opposite ends of the assembled region of *4*. These females were crossed *w*^{1118}; *sv*$^{spa\text{-}pol}$ males and the progeny were scored for the poliert eye phenotype associated with *sv*$^{spa\text{-}pol}$ homozygosity and the *w*$^{+m}$ of the *PBac* transgene. Although both the *M*{*UASp::mei-41*} and *P*{*matα4::GAL4-VP16*} transgenes also carry a *w*$^{+m}$, both confer only mild eye coloration, so the strong red-eye phenotype of *PBac*{*y*$^{+}$ *w*$^{+m}$}(101F) is easily discerned.

Genetic distances, expressed here in centiMorgans (cM) rather than "map units", as is traditionally used in *Drosophila*, were calculated using the equations of Stevens (Stevens 1936). Crossover density was calculated by dividing *cM* by the distance between markers (rounded to nearest 10 kb), using *Drosophila melanogaster* reference genome release 6.12 with transposable elements excluded, as described in Hatkevich *et al.* (Hatkevich *et al.* 2017). Including transposable elements in distances did not change any conclusions (see Tables 3.6a and 3.6b).

The coefficient of coincidence (*c*) is calculated as $c = \frac{(d)(n)}{(a)(b)}$, where *a* and *b* are the number of single-crossover progeny in two intervals being compared, *d* is the number of double-crossover (DCO) progeny, and *n* is the total progeny scored. This is equivalent to observed DCOs divided by expected DCOs if the two intervals are

Genotype	Interval on Chromosome *2*					
	I	**II**	**III**	**IV**	**V**	**I - V**
	Genetic Size (cM ±95% CI)					
WT	4.74 ±0.64	7.51 ±0.80	27.29 ±1.35	4.55 ±0.52	1.73 ±0.39	45.81 ±0.90
mei-41	1.29 ±0.25	1.70 ±0.28	7.14 ±0.57	3.87 ±0.43	1.05 ±0.23	15.06 ±0.79
mei-9 mei-41	2.46 ±0.93	1.13 ±0.64	6.80 ±1.52	3.87 ±1.16	1.32 ±0.69	15.58 ±2.18
mei-9	0.25 ±0.20	0.46 ±0.27	1.64 ±0.51	0.33 ±0.23	0.08 ±0.11	2.75 ±0.65
Mb w/o TEs	2.312	2.004	9.006	5.639	9.438	28.399
WT	2.05 ±0.28	3.75 ±0.40	3.03 ±0.15	0.81 ±0.09	0.18 ±0.04	1.61 ±0.05
mei-41	0.56 ±0.09	0.86 ±0.14	0.79 ±0.06	0.69 ±0.08	0.11 ±0.03	0.53 ±0.03
mei-9 mei-41	1.06 ±0.40	0.57 ±0.33	0.75 ±0.16	0.69 ±0.19	0.14 ±0.07	0.55 ±0.08
mei-9	0.11 ±0.09	0.23 ±0.14	0.18 ±0.05	0.06 ±0.04	0.01 ±0.01	0.10 ±0.03
Mb w/ TEs	2.394	2.052	9.292	6.253	11.724	31.715
WT	1.98 ±0.27	3.66 ±0.39	2.94 ±0.15	0.73 ±0.10	0.15 ±0.04	1.44 ±0.04
mei-41	0.54 ±0.10	0.83 ±0.14	0.77 ±0.06	0.62 ±0.08	0.09 ±0.02	0.47 ±0.02
mei-9 mei-41	1.03 ±0.39	0.55 ±0.31	0.73 ±0.16	0.62 ±0.19	0.11 ±0.06	0.49 ±0.07
mei-9	0.10 ±0.08	0.22 ±0.13	0.18 ±0.06	0.05 ±0.03	0.01 ±0.01	0.09 ±0.02

Genotype	Interval on Chromosome *X*					
	I	**II**	**III**	**IV**	**V**	**I - V**
	Genetic Size (cM ±95% CI)					
WT	10.09 ±1.26	20.00 ±1.68	10.41 ±1.28	10.92 ±1.31	11.42 ±1.34	62.84 ±2.03
mei-41	4.40 ±0.67	8.87 ±0.77	3.34 ±0.49	4.39 ±0.56	6.07 ±0.65	27.09 ±1.21
Mb w/o TEs	5.018	5.089	2.732	3.385	5.568	21.792
WT	2.01 ±0.25	3.93 ±0.33	3.81 ±0.47	3.23 ±0.39	2.05 ±0.24	2.88 ±0.09
mei-41	0.88 ±0.11	1.74 ±0.15	1.22 ±0.18	1.30 ±0.17	1.09 ±0.12	1.24 ±0.05
Mb w/ TEs	5.295	5.233	2.810	3.521	6.291	23.150
WT	1.91 ±0.24	3.82 ±0.32	3.71 ±0.46	3.10 ±0.37	1.82 ±0.22	2.71 ±0.08
mei-41	0.84 ±0.11	1.69 ±0.14	1.19 ±0.17	1.25 ±0.16	0.96 ±0.10	1.17 ±0.05

Table 3.6. Genetic distances and crossover densities. The top section of each table gives calculated genetic distances (in cM, with 95% confidence intervals (CI); see Materials and Methods) for the five intervals on *2L* (see Table 3.3) and *X* (see Table 3.4). The rightmost column has the summed distance across all five intervals. The lower two sections give crossover density (cM/Mb) calculated without including transposable elements (middle) or including transposable elements (bottom). Transposable element lengths are from the *Drosophila melanogaster* reference genome and are not necessarily the same in the chromosomes we used.

independent (no interference). Interference (*I*) is 1-*c*. Thus, *I* = 0 in the absence of interference and *I* = 1 if there is complete positive interference (no DCOs observed).

The centromere effect was quantified as in Hatkevich *et al.* (Hatkevich *et al.* 2017). The definition parallels that of *I*: *CE* = 1-(*O*/*E*), where *O* is the number of crossovers observed and *E* is the number expected based on the average crossover density across the entire region assayed. *CE* therefore describes the deviation in crossover density in any interval from the mean density across all intervals.

For crossover assurance, we obtained the expected number of meiosis in which a given region of the genome (*X* or *net–cn*) had no crossovers (E_0) from the Poisson distribution, using mean number of crossovers in that region as the average rate of success. To convert observed crossover classes (parental, single, double, and triple crossover) to bivalent exchange classes (E_0, E_1, E_2, E_3) we used the method of Weinstein (Wweinstein 1936). This method accounts for the fact that an E_1 "tetrad" gives two crossover chromatids and two parental chromatids, so the probability of recovering the crossover in the progeny is 0.5. Weinstein tested models with and without sister chromatid exchange and with and without chromatid interference (*i.e.*, whether the chromatids involved in the two crossovers of a DCO are independent of one another). We used the model that he found to be the best fit to two large *Drosophila* datasets: no sister chromatid exchange and no chromatid interference.

X nondisjunction was scored by crossing virgin mutant females of the appropriate genotypes to *y sc cv v g f / Dp(1:Y)B*^{S} males. Exceptional progeny for *X* nondisjunction events originate from diplo-*X* and nullo-*X* ova, resulting in *XXY* (Bar-eyed females) and

XO (wild-eyed males) progeny, respectively. Numbers of exceptional progeny were doubled to account for those that do not survive to adulthood (*XXX* and *YO*).

Statistical analyses

For *cM* and *c* (and therefore *I*), 95% confidence intervals were calculated as $\pm 1.96\sqrt{V(x)}$, where *V(x)* is the variance of parameter *x*. $V(cM) = \frac{(cM)(1-cM)}{n}$ and $V(c) = \left(\frac{c}{n}\right)\left(\frac{1-ca-cb-cab+2c^2ab}{ab}\right)$ (Stevens 1936). For nondisjunction, 95% confidence intervals and comparisons of rates across genotypes followed the statistical methods developed by Zeng *et al.* (Zeng *et al.* 2010).

For between-genotype comparisons of interference we conducted χ^2 tests on 2-by-2 contingency tables of observed and expected DCOs for each genotype. A 2-by-2 table is appropriate for counts of events that are positive integer values and for which there is an expectation under the null hypothesis that mutant and wild type have the same levels of interference given their levels of recombination. This expected number of DCOs is derived by applying a model of the frequency of double crossovers under no interference. Since the data do not have covariates or repeated measures, a χ^2 test is the most straightforward. We applied Yates' continuity correction because of low counts in some categories. A similar argument holds for the centromere effect and assurance. For assurance, we compared observed and expected E_0 and $E_{>0}$ classes. χ^2 tests were conducted using the GraphPad QuickCalcs online tool (https://www.graphpad.com/quickcalcs/contingency1.cfm).

CHAPTER 4

CONCLUDING REMARKS

Overview

In this dissertation I sought to exploit crossover patterning differences between the canonical meiotic Class I and Class II (now more specifically designated as crossovers generated outside the canonical meiotic pathway) pathways to determine a temporal role of the *Drosophila* ATR ortholog, *mei-41*, during meiotic recombination. Although *mei-41* was initially characterized as a meiotic mutant in 1972 (Baker and Carpenter 1972), these alleles were either hypomorphic or separation-of-function due to the maternal-effect embryonic lethality phenotype of null alleles (Sibon *et al.* 1999). Therefore, current literature focused on exploring the mitotic DSBR and checkpoint functions of *mei-41*. The creation of a transgenic *mei-41* meiotic recombination null allowed us to better understand the impact of Mei-41 on crossover control phenomena. Our findings allowed us to separate the establishment of the centromere effect from crossover assurance and crossover interference, a result that agrees with current models of meiotic crossover patterning (Wang 2015). This has work further implications beyond *Drosophila*, as aberrant crossover patterning leads to increased chromosome disjunction in humans, resulting in common newborn syndromes such as trisomy 21 (Lamb *et al.* 1996; Koehler *et al.* 1996).

Highlighted Findings

We created a *mei-41* meiotic recombination null, where Mei-41 is absent prior to and throughout meiotic recombination in the germarium but present at later oogenic stages (Sanghavi *et al.* 2013), thus fulfilling the requirement for maternally-loaded embryonic Mei-41 to avoid maternal embryonic lethality. This allowed for crossover patterning analysis utilizing progeny from *mei-41* null mothers for the first time. Compared to hypomorphic mutants, the *mei-41* null retained the polar effect observed on *2L*, but displays more severe crossover reduction and *X*-nondisjunction phenotypes. Of greater note, however, is that the *mei-41* null retains a strong centromere effect despite the significant reduction in crossover interference and assurance.

Previous research in *Drosophila Blm* mutants shows all three patterning phenotypes are lost and resulting crossovers do not rely in the putative meiotic resolvase Mei-9, suggesting Blm is required for entry into the canonical, Class I pathway (Hatkevich *et al.* 2017). However, this work establishes that crossover assurance and crossover interference are separable from the centromere effect in *mei-41* nulls, and we hypothesize that crossover patterning is established in a stepwise manner, starting with the centromere effect (Figure 3.3). Additionally, resulting crossovers do not require Mei-9, suggesting that these mutants establish the centromere effect within the canonical meiotic pathway, but switch to an alternate pathway for all subsequent crossover patterning and resolution (see Chapter 3 Discussion). While its mechanism remains unknown, previous research into the mitotic roles of Mei-41 demonstrate its involvement in SDSA annealing and ligation (LaRocque *et al.* 2007). Additional work by Holsclaw and Sekelsky posits that the annealing of

complementary sequences is catalyzed by Marcal1 via Mei-41 (Holsclaw and Sekelsky 2017). This suggests that Mei-41 may phosphorylate substrates involved in second-end capture prior to the formation of dHJs that are then resolved by Mei-9. In the absence of Mei-41, the invading 3' homolog may be disassociated from the D loop and repaired as an NCO via Blm within a mitotic context.

Future Directions

While this dissertation establishes the groundwork for the separation of the centromere effect from other crossover patterning processes, future experiments may confirm our observations and shed additional light on mechanism. One intriguing result from the original Carpenter and Baker paper is that a second allele of *mei-41*, now known as *mei-41*^{2}, resulted in an increase in pericentromeric COs relative to wild-type, suggesting this allele was a separation-of-function mutant. Unlike the original *mei-41*^{1} mutant, *mei-41*^{2} remains available as a stock, but the nature of the mutation has not yet been characterized. It is possible that the nature of the *mei-41*^{2} mutation may be antagonistic to other factors important to centromere effect establishment. Sequencing may reveal structural insights into the nature of this mechanism in retaining the centromere effect.

Another important question to address regards whether or not meiotic patterning defects seen in the *mei-41* null operate independently of its checkpoint functions. Work from the McKim lab shows that Mei-41 has a role in meiotic DSB repair outside of its role as a checkpoint protein (Joyce *et al.* 2011). Alternatively, disruption of the ATR-CHK1 pathway results in a complete inability to synapse homologs in mouse spermatocytes via failure to load RAD51 (Pacheco *et al.* 2017). To determine if the

defects in meiotic patterning observed in *mei-41* mutants are accomplished through the checkpoint pathway, comparing meiotic patterning defects seen in downstream checkpoint targets *grp*/CHK1 *lok*/CHK2 double mutants to *mei-41* single mutant nulls may help resolve this question.

Perhaps the most important question to address is why the centromere effect is retained in *mei-41* nulls. The centromere effect has been attributed to higher-order chromatin structure at the centromere, and our data, combined with data from Hatkevich *et al.* (Hatkevich *et al.* 2017), demonstrate its establishment precedes crossover interference and assurance. Studies in *S. cerevisiae* show the Ctf19 kinetochore subcomplex is responsible for both the inhibition of DSBs and the inhibition of homolog interactions in pericentromeric regions via cohesin enrichment (Choo 1998; Vincenten *et al.* 2015). Additionally, the budding yeast ATR ortholog, Mec1, has been shown to promote interhomolog recombination via the SC axial element protein Hop1 (Grushcow 1999; Carballo 2008). However, in *Drosophila,* NCO repair events are evenly distributed along euchromatin (Comeron *et al.* 2012; Miller *et al.* 2016). This suggests that the *Drosophila* centromere effect is not established due to a lack of DSB induction, but that potential CO precursors are preferentially repaired using the sister template, a hypothesis corroborated by the fact that cohesin levels in *S. cerevisiae* dictate template choice in DSBR (Covo *et al.* 2010). Comparative staining of the cohesin subunit Smc1 between *Blm* and *mei-41* nulls would yield preliminary data regarding the role of cohesin and centromere effect establishment, as cohesin enrichment may be lost in *Blm* nulls but retained in *mei-41* nulls. Additionally, sister-chromatid exchange assays and

heteroduplex DNA analysis in these regions may resolve questions regarding template choice.

In conclusion, the work presented here reveals not only an intriguing role of Mei-41 in crossover patterning, but also creates an imperative for studying centromere effect establishment in both *Drosophila* and other organisms to better understand the mechanism behind proximal NDJ events leading to human aneuploidy, gamete dysfunction, and miscarriage.

APPENDIX

NUCLEAR FALLOUT IN *Blm* MUTANT PROGENY: A PROLONGED EXERCISE IN DEVELOPMENTAL NIHILISM

Preface

The following represents a compilation of work done by former SPIRE Postdoctoral Fellow, Dr. Eric Stoffregen, and myself on nuclear defects in *Drosophila melanogaster* embryos lacking maternally-loaded Blm, and serves as a repository of our collected data for future reference. A brief review of the BLM helicase and Dr. Stoffregen's previous work are outlined in the Introduction, while subsequent experiments performed by myself are listed in the Results and Discussion.

Introduction

Loss of the RecQ helicase BLM results in Bloom syndrome (BS), a rare disorder characterized by proportional dwarfism, photosensitivity, immune deficiencies, and a wide array of early-onset cancers due to high levels of genome instability (German 1993; Ellis *et al.* 1995; Hickson 2003). Resulting BS cells display hyper-recombination between sister chromatids and homologous chromosomes, in addition to chromosome breaks, deletions, and rearrangements (Tachibana *et al.* 1996; Sonoda *et al.* 1999; Gonzales-Barrera *et al.* 2003). Due to these phenotypes, *in vitro* studies attributed anti-recombinase functions to BLM and demonstrated that the helicase preferentially unwinds/migrates D loop and HJ-containing HR recombination intermediates, thereby promoting branch migration to prevent promiscuous recombination events (Karow *et al.* 1997; van Brabant *et al.* 2000; Karow *et al.* 2000). In *Drosophila melanogaster, Blm* encodes the BLM ortholog (formerly known as *mus309*), and flies carrying null alleles

are defective in SDSA-mediated HR following DSB induction. Resulting phenotypes display large deletions flanking the DSB break site, a phenotype also seen in BS cell lines (Boyd 1981; Kusano *et al.* 2001; Gaymes *et al.* 2002; Adams *et al.* 2003).

However, BLM also exhibits pro-recombinase functions, as SDSA-impaired *Drosophila Blm* mutants show a decrease in synthesis length, implicating a role for the protein in unwinding DNA or D loop dissociation (Adams *et al.* 2003). Subsequent experiments in *Drosophila* demonstrate that *Blm* mutant phenotypes are not caused by an inability to initiate SDSA repair synthesis, but are instead a result of *spn-A*/Rad51-mediated invasion, resulting in deletions when Blm is absent and unable to unwind the invading strand from the D loop (McVey *et al.* 2004a; McVey *et al.* 2004b). Corroborating evidence in other organisms shows that BLM interacts with homologous repair proteins Rad51, replication protein A, and Mlh1, consistent with a role in DSB repair and BS cell phenotypes (Brosh *et al.* 2000; Pedrazzi *et al.* 2001; Wu *et al.* 2001; Hu *et al.* 2005). Subsequent biochemical studies confirmed both anti- and pro-recombinase functions of BLM at different stages of HR, with BLM inhibiting DNA strand exchange at D loops by dismantling Rad51 coated ssDNA (HR suppression) while also promoting D loop unwinding and subsequent DNA repair synthesis (HR stimulation) (Bugreev *et al.* 2007).

In *Drosophila*, *Blm* mutants exhibit maternal embryonic lethality, resulting in semi-sterile mothers, as only 4% of progeny reach adulthood (referred to as *Blm* mutant progeny). This phenotype is attributed to defects in the early embryo during rapid NCs throughout syncytial development (refer to Chapter 2 for additional information regarding early embryogenesis in *Drosophila*), resulting in anaphase bridges and

asynchronous mitoses (McVey 2007). Nuclear damage sustained during these early NCs exit the cell cycle and fall from the cortex of the syncytial blastoderm to the interior, often dragging neighboring nuclei with them and resulting in the 'nuclear fallout' phenotype. These fallen nuclei do not become somatic nuclei and therefore do not contribute to further embryonic development (O'Dor *et al.* 2006).

Previous work utilizing electron microscopy shows that facilitating rapid embryonic NCs requires a substantial increase in firing replication origins, with 1 fork per 10 kb of DNA, resulting in several instances of fork convergence and potential fork stalling (Kriegstein and Hogness 1974). As Blm has been implicated in the recovery of stalled or damaged replication forks and plays a role in bypassing DNA damage resulting in fork stalling or collapse, lack of maternally loaded Blm may result in unresolved joint molecule or secondary structure formation leading to chromosome fusions (Sengupta *et al.* 2003; Sengupta *et al.* 2004; Ralf *et al.* 2006). Therefore, Dr. Eric Stoffregen hypothesized that maternally-deposited Blm is required to respond to replication challenges during early NCs. Subsequent immunofluorescence of nuclear defects in early embryos from *Blm* mutant mothers replicate previously reported *Blm* phenotypes (McVey *et al.* 2007), with large patches of mitotic asynchrony or nuclear fallout by NC 12-14 (Figure 5.1), likely resulting in embryonic inviability.

Of the *Blm* mutant progeny that survive to adulthood, adults exhibit a significant sex bias of females over males relative to wild-type controls ($n = 3564$; $p < 0.0001$) (Figure 5.2A). As the *Y* chromosome of *Drosophila* is almost entirely heterochromatic (~40 Mb) compared to the heterochromatin on the *X* chromosome (~20 Mb), *XY* males contain 50% more (60 Mb) heterochromatin than *XX* females (40 Mb) (Ashburner 2005).

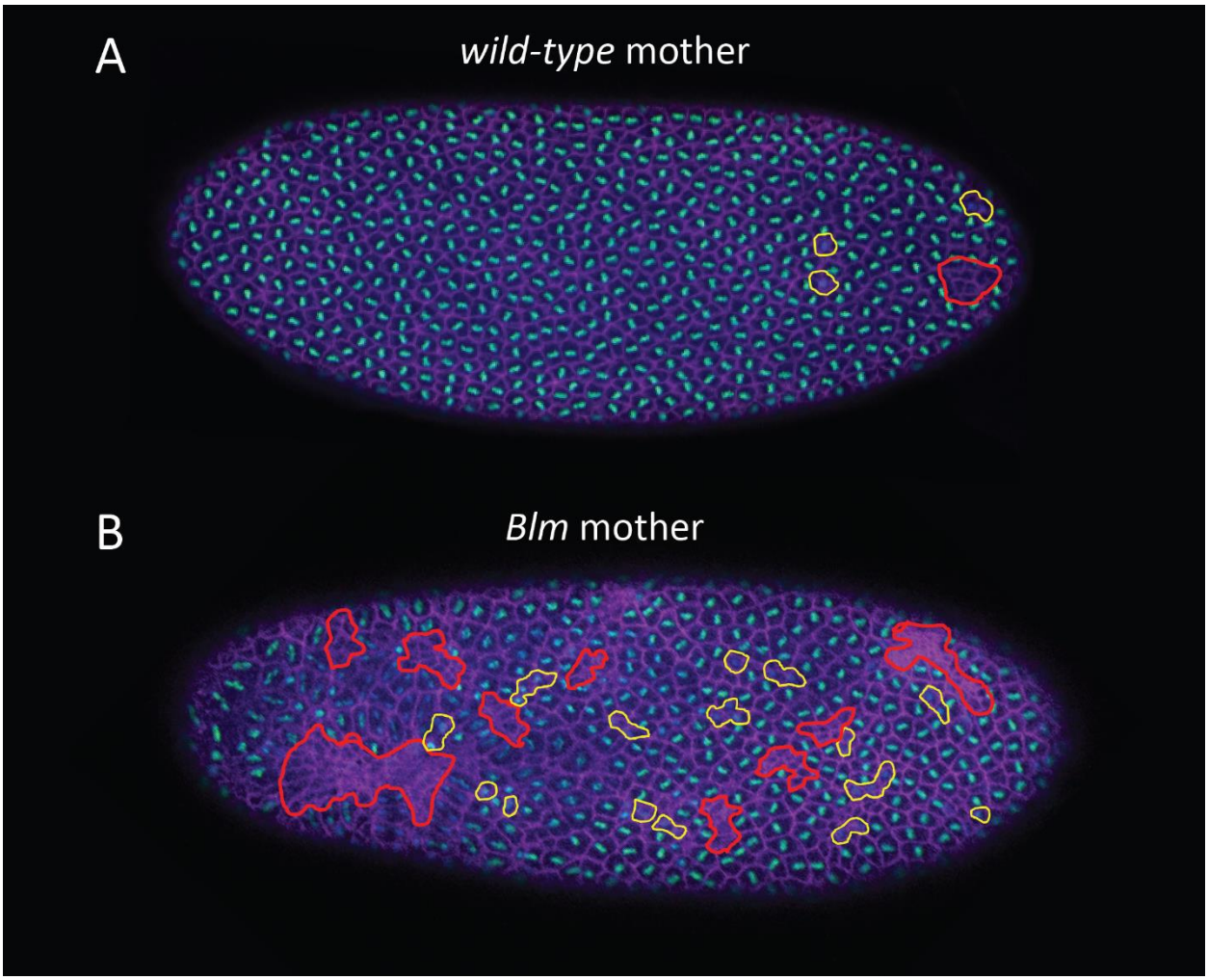

Figure 5.1. Early embryos lacking maternally loaded *Blm* exhibit nuclear defects. Syncytial blastoderm prior to NC 14 of wild-type (A) and *Blm* (B) embryos. Phosphorylated histone 3 (α-pH3, green) marks mitosis; phosphorylated tyrosine (α-pTyr, purple) demarcates actin cages; DNA (DAPI, blue). Mitotic asynchrony outlined in yellow, nuclear fallout outlined in red. (A) Embryos from wild-type mothers undergo mitosis synchronously, though some mitotic asynchrony and acute, localized nuclear fallout is visible but not lethal. (B) Embryos from *Blm* mutant mothers show extreme levels of nuclear damage relative to wild-type, including numerous instances of mitotic asynchrony and several large regions of nuclear fallout contributing to early embryonic death. Microscopy and figure by E.S and J.S.; edited for presentation by M.B.

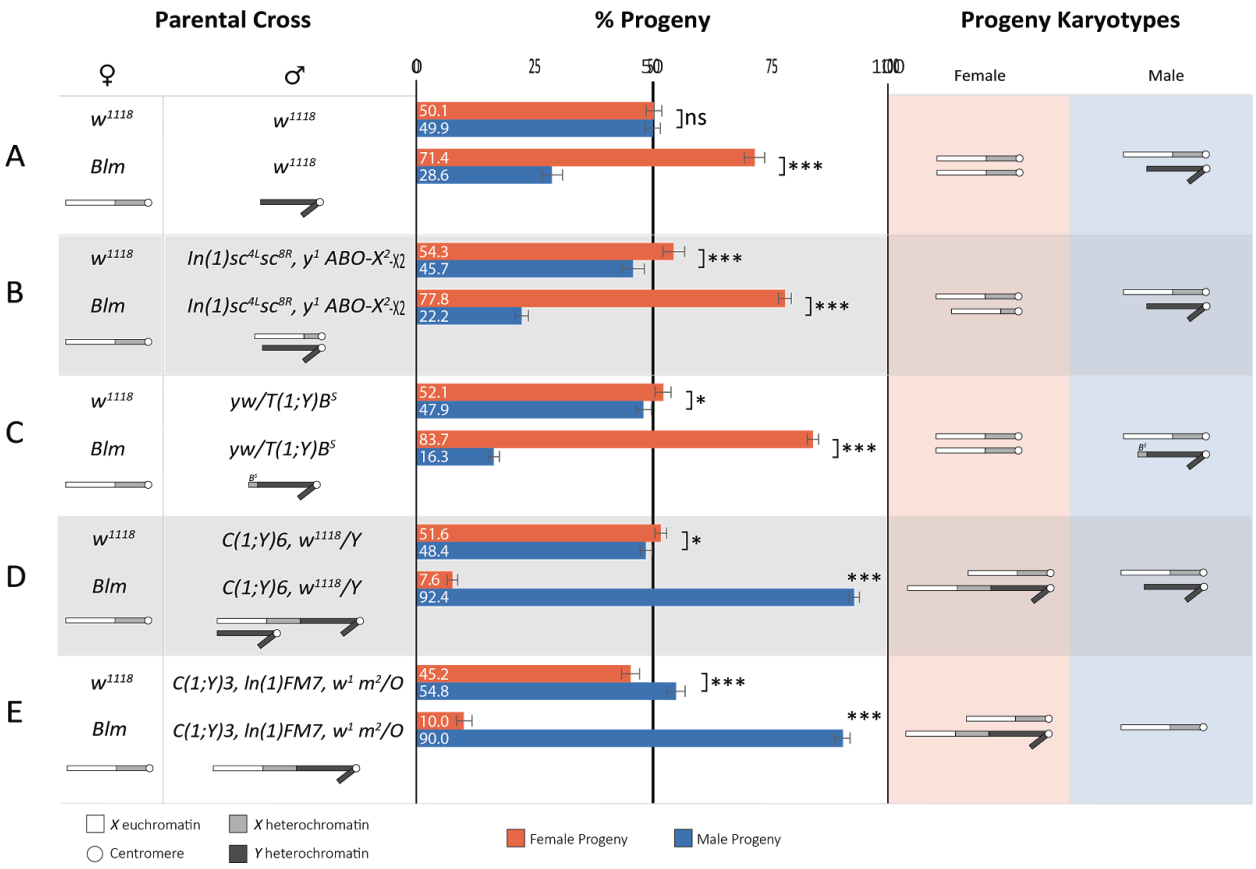

Figure 5.2. *Blm* mutant progeny survival inversely correlates with increased heterochromatin. Left, parental genotypes and corresponding sex chromosome karyotype; middle, percent adult progeny survivors divided by sex (actual percentage in white numbers); right, sex chromosome karyotypes of adult progeny survivors. (A) Control female (w^{1118}) and heteroallelic *Blm* female nulls (*N1/D2*) crossed to control male (w^{1118}) (*n* = 3564 and 1703, respectively). (B) Control and *Blm* females crossed to males carrying a ⅔ deletion of *X* heterochromatin (n = 1746 and 3748, respectively). (C) Control and *Blm* females crossed to males carrying additional *X* heterochromatin and euchromatin on the *Y* chromosome (*n* = 3702 and 3734, respectively). (D) Control and *Blm* females crossed to males carrying a copy of the *Y* chromosome on the *X* chromosome (*X-Y* compound chromosome) in addition to a separate *Y* chromosome (*n* = 2626 and 1343, respectively). (E) Control and *Blm* females crossed to males carrying the *X-Y* compound chromosome but lacking an additional sex chromosome (*n* = 3702 and 3734, respectively). Statistical significance determined via χ2 tests on observed progeny sex versus expected progeny sex, if expected sex ratio is 1:1 (ns, $p > 0.05$; *$p > 0.01$; ***$p > 0.0001$; bars represent 95% confidence interval). Data collected by E.S.; statistics and figure by M.B.

Utilizing a variety of compound sex chromosomes resulting in increases or decreases in progeny heterochromatin, Stoffregen showed that increasing heterochromatin in *Blm* mutant progeny resulted in poorer survival (Figure 5.2B-E).

However, heterochromatin remains in a naïve state until NC 12, and major markers of heterochromatin, such as heterochromatin protein 1 (HP1), are not abundant until NC 14 (Shermoen *et al.* 2010; Li *et al.* 2014). Additionally, constitutive *Drosophila* heterochromatic regions are primarily composed of satellite sequences and transposable elements, including the 359-bp repeat, to which HP1 binds following a dramatic increase in the repressive histone modifications H3K9me2 and H3K9me3 during interphase of NC 14 (Bannister *et al.* 2001; Lachner *et al.* 2001; Nakayama *et al.* 2001; Elgin and Reuter 2013; Yuan and O'Farrell 2016). Therefore, the heterochromatin state itself is unlikely to be the cause of nuclear defects seen in early *Blm* mutant embryos, as observed defect severity is indicative of beginning several NCs earlier. Subsequent experiments performed by Stoffregen showed that sex bias with increased repetitive DNA was not the result of DSB repair defects, as sex bias ratios were ameliorated in mothers homozygous for the *N2 Blm* allele, which is deficient for SDSA but retains the helicase domain (McVey *et al.* 2007). Alternatively, progeny from *Blm* mutant females heterozygous for *DNApol-α*, which impedes DNA replication, exhibit a more severe sex bias than the single mutant, suggesting that the role of Blm in the early embryo is responding to replication challenges. Together, nuclear defects may be due to some property of the heterochromatic DNA sequence itself, such as repetitive sequence load that requires Blm to bypass. As BLM has been implicated at sites of fork-stalling or G-quadruplexes (Ralf *et al.* 2006; Sun *et al.* 1998), embryos lacking the

maternally-loaded Blm helicase may result in an inability to facilitate replication through these regions.

Results and Discussion

Heterochromatin localization is not temporally altered in Blm *mutant embryos*

As HP1 and corresponding repressive histone modifications are not observed in wild-type embryos until NC 14, we wanted to determine if these major heterochromatic markers were temporally wild-type in *Blm* mutant embryos and therefore not the source of early nuclear defects. Utilizing an antibody against H3K9me2, which is not abundant until NC 14, both control (w^{1118}) and *Blm* mutant embryos lack H3K9me2 localization until after cellularization occurs at NC 14 (Figure 5.3), suggesting that constitutive heterochromatin state is not the source of observed genomic instability.

Sex bias does not manifest in the early embryo

Embryos from Blm mutant mothers exhibit a severe sex bias ratio, but it is unknown at which stage this bias manifests. Due to the severe nuclear phenotypes seen in *Blm* mutant embryos and previously reported embryonic gastrulation failure (McVey *et al.* 2007), we wanted to determine when sex bias manifests during embryogenesis. Embryos from *Blm* mutant mothers (generated by the Reaper Assay carrying *P{sxl::eGFP}*; see Materials and Methods) crossed to isogenized w^{1118} males were visualized via confocal microscopy. As *sxl::eGFP* results in sex-specific GFP expression, embryos exhibiting green fluorescence are marked as female before sex-specific morphological differences are evident (Schütt and Nothiger 2000; Thompson *et al.* 2004) (Figure 5.4). Surprisingly, the number of post-gastrulation embryos from *Blm*

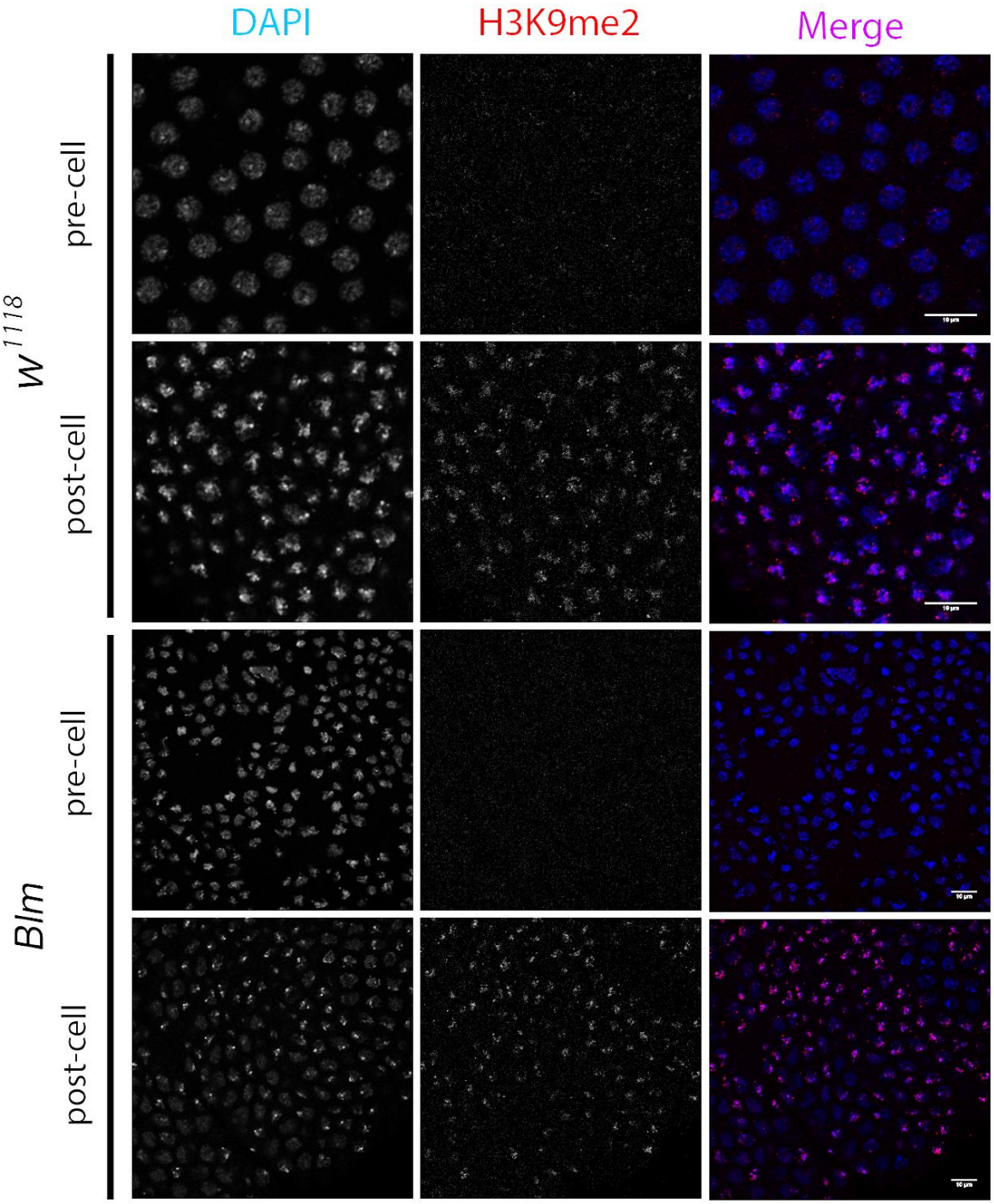

Figure 5.3. H3K9me2 localizes to nuclei following cellularization at NC 14 in both control and *Blm* mutant embryos. Analysis of control (top) and *Blm* (bottom) mutant embryos. Embryos were divided into pre-cellularization at NC 14 (pre-cell) and post-cellularization at NC 14 (post-cell). Left column shows DNA (DAPI); middle column shows H3K9me2 (α-H3K9me2); right column shows merged (DNA, blue; H3K9me2, red). Scale bars represent 10 μm.

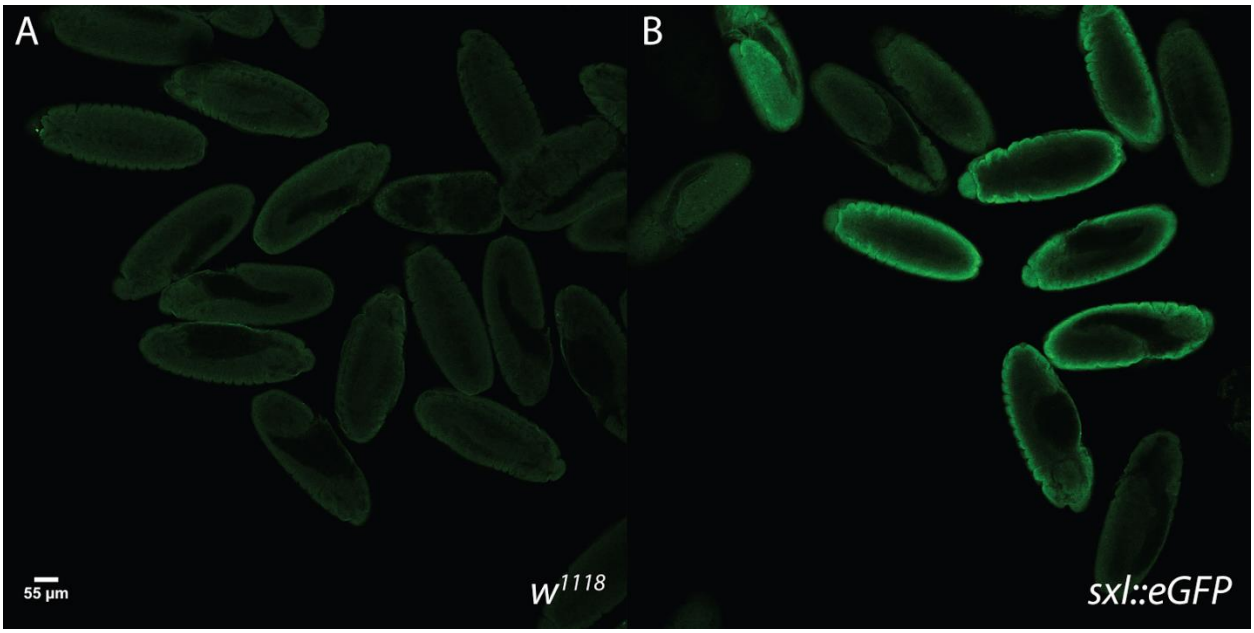

Figure 5.4. Embryonic sex differentiation using *sxl::eGFP*. (A) Control embryos (w^{1118}) lack sex-based fluorescence. (B) Sex ratios from embryos homozygous for *sxl::eGFP* can be quantified based on *eGFP* expression. Scale bar represents 55 µm. See Materials and Methods for further information.

mutant mothers was much higher than previously reported (McVey *et al.* 2007), though a fraction of these embryos exhibited developmental delays or lacked post-gastrulation morphology indicative of early embryonic death.

Of the *Blm* mutant embryos at the appropriate stage, there was no significant difference between morphologically wild-type male (66) and female (71) embryos at 8.5 hours post collection, when *sxl::eGFP* expression is optimal ($p > 0.669$, $\chi 2$ test) (Thompson *et al.* 2004), suggesting that early embryonic defects do not contribute the observed sex bias ratio in adults, or that sex bias cannot yet be statistically detected. Subsequent experiments to determine if sex bias manifested at later embryonic stages were unsuccessful, as eGFP fluorescence had degraded (data not shown).

Blm *embryos exhibit a slow decline in survivability following gastrulation*

Due to the unexpected number of embryos that survived post-gastrulation, we

wanted to determine the rate of embryonic death in *Blm* mutant embryos. Over half of all embryonic death was observed within the first 3-hour window of embryogenesis, with survival decreasing at a much slower rate over the course of embryogenesis (Figure 5.5). By 21 hours, only 12% of embryos displayed wild-type morphology, suggesting only a small fraction make it to hatching. Therefore, Blm appears to play a major role in the early embryo. Subsequent death seen in later stages may be the result of earlier defects. Additionally, as zygotic gene expression begins following NC 14, one copy of wild-type Blm (from the father fly) may help ameliorate Blm-related defects in these later stages.

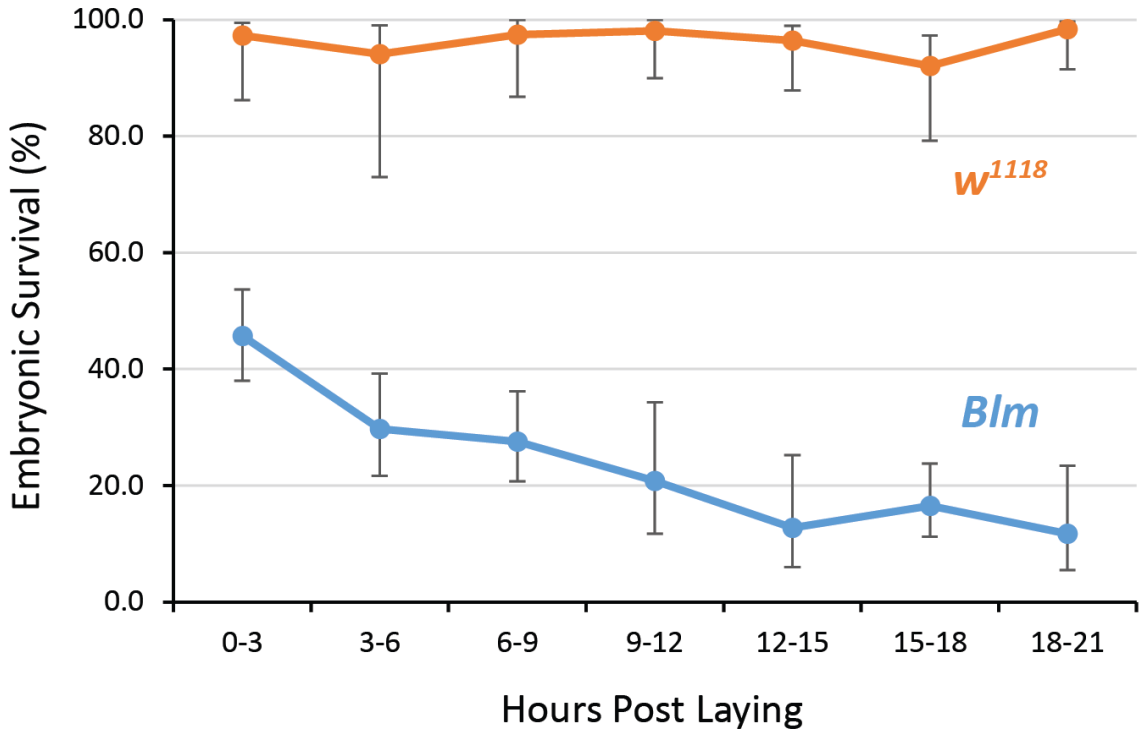

Figure 5.5. Half of all embryos from *Blm* mutant mothers die prior to gastrulation. Between 0 to 3 hours post laying, only 45.7% of all embryos observed did not exhibit canonical *Blm* nuclear defects resulting in likely embryonic inviability. Survival at the following time point (3 to 6 hours post laying) dropped to 29.7%, which may include developmentally delayed embryos attempting and failing to gastrulate. Survivability decreases throughout the remainder of embryogenesis (with the exception of 15 to 18 hours), with only 11.8% of embryos hatching within 18 to 21 hours. Bars represent 95% confidence intervals.

Genotype	Eclosed Female (n)	Eclosed Male (n)
N1/N1	6.40 (11)	3.90 (2)
D2/N1	25.1 (43)	17.6 (9)
N1/TM6B	41.5 (71)	54.9 (28)
D2/TM6B	26.9 (46)	23.5 (12)
w^{1118}/w^{1118}	52.2 (423)	47.8 (388)
N1 or D2 / w^{1118}	68.8 (696)	31.2 (315)

TABLE 5.1. Zygotic expression of wild-type *Blm* yields higher eclosion frequencies. Adult progeny heterozygous for wild-type *Blm* exhibit higher eclosion frequencies than adult progeny homozygous or heteroallelic for mutant *Blm* ($p < 0.0001$ for combined sexes, $\chi 2$ test on observed heterozygous and homozygous/heteroallelic adults versus expected heterozygous and homozygous/heteroallelic adults, if expected ratios are Mendelian 1:1). Genotype shows maternal contribution left of slash; numbers listed are percentages per sex and counts (*n*). Last two rows represent progeny from two separate control crosses and replicate data originally obtained from E.S.

Zygotic expression of wild-type Blm *ameliorates the pharate lethality phenotype*

To analyze the role of zygotic gene expression, *Blm* mutant mothers were crossed to males heterozygous for the *N1* allele of *Blm* (*N1*/*TM6B*). Progeny homozygous (*N1*/*N1*) or heteroallelic (*N1*/*D2*) for *Blm* failed to eclose at statistically higher rates ($p < 0.0001$ for both sexes) than progeny carrying a one wild-type allele on the *TM6B* balancer (*N1*/*TM6B* or *D2*/*TM6B*), indicating zygotic expression of Blm may rescue lethality throughout development (Table 5.1).

Interestingly, out of the 222 flies that made it to adulthood, an additional 250 flies died as pharate adults, suggesting that death induced by lack of Blm may not be restricted to the embryo, but may instead be a prolonged process throughout all of development. To address this, we repeated the experiment and divided pharate adults by genotype. As the *TM6B* balancer carries the *tubby* (*Tb*) mutation, *N1*/*TM6B* and

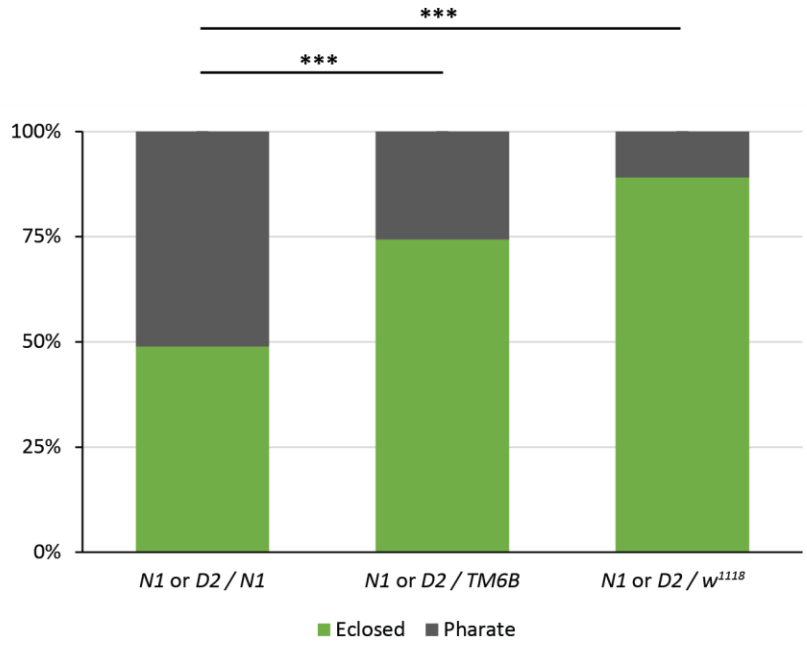

Figure 5.6. Zygotic expression of wild-type *Blm* inversely correlates with pharate lethality. Adult progeny heterozygous for wild-type *Blm* exhibit are less likely to die as a pharate adults compared progeny homozygous or heteroallelic for mutant *Blm*. *Blm* alleles balanced over TM6B fare worse than *Blm* alleles balanced over wild-type chromosome *III* (from w^{1118}). Statistical significance determined via two-tailed Fisher's exact test on heterozygous (*Blm* allele over TM6B or w^{1118}) and homozygous/heteroallelic eclosed adults versus heterozygous (*Blm* allele over TM6B or w^{1118}) and homozygous/heteroallelic pharate adults (***$p > 0.0001$). See Table 5.2 for counts and additional information.

Genotype	Eclosed Female (*n*)	Eclosed Male (*n*)	Total Eclosed (*n*)	Total Pharate (*n*)
N1/N1	8.77 (20)	0.44 (1)	48.9 (69)	51.1 (72)
D2/N1	16.7 (38)	4.39 (10)		
N1/TM6B	30.7 (70)	9.20 (21)	74.3 (159)	25.7 (55)
D2/TM6B	20.6 (47)	9.20 (21)		
$N1/w^{1118}$	35.3 (130)	10.9 (40)	89.1 (368)	10.9 (45)
$D2/w^{1118}$	36.9 (136)	16.9 (62)		
$w^{1118}/N1$	35.3 (201)	33.5 (191)	99.1 (570)	0.90 (5)
$w^{1118}/TM6B$	16.5 (94)	14.7 (84)		
w^{1118}/w^{1118}	47.7 (294)	52.3 (322)	99.2 (616)	0.80 (5)

TABLE 5.2. Zygotic expression of wild-type *Blm* inversely correlates with pharate adults. Adult progeny heterozygous for wild-type *Blm* are less likely to die as a pharate adults compared to progeny homozygous or heteroallelic for mutant *Blm*. Genotype shows maternal contribution left of slash; numbers listed are percentages per cross and counts (n). Last three rows represent progeny from control crosses, yielding < 1.0% pharate adults. Refer to Figure 5.6 for statistical analysis.

D2/*TM6B* pupal cases are ‘tubby’ compared to *N1*/*N1* or *N1*/*D2*, allowing analysis between progeny that are heterozygous and homozygous for *Blm* before eclosion occurs. Again, homozygous progeny had a significant ($p > 0.0001$, two-tailed Fisher’s exact test) increase in the frequency of pharate lethal adults compared to the heterozygous progeny balanced with *TM6B*. Additionally, *Blm* mutant mothers crossed to w^{1118} controls exhibited less pharate lethal adults compared to mothers crossed to males containing the *TM6B* balancer, most likely due to the inherent sickliness of balancer chromosomes.

As Blm appears to play a role past embryogenesis, it is possible that sex bias manifests during pupation. To determine sex ratios, we utilized primers against the Y chromosome from collected pharate lethal adults. Unfortunately, DNA fidelity from these adults was variable and the PCR was uninformative (data not shown). This is most likely due to the fact that collection occurred 2 days following all sibling eclosion to account for developmental delays, resulting in tissue desiccation.

Future Directions

Our collected data show that, while most lethality from *Blm* mutant mothers occurs during early embryogenesis, lethality is not restricted to embryogenesis and instead appears to be a prolonged process throughout all of development. As there is an 8% discrepancy between *Blm* mutant progeny surviving embryogenesis and eclosion (McVey *et al.* 2007), sex bias may manifest during larval stages or later. Preliminary data from hatch rate experiments and PCR suggest sex bias does not manifest during early larval stages, but too few larvae were collected for statistical power. Therefore, to determine if sex bias manifests in larval stages, *Blm* mutants carrying *yellow* (*y*) and

white (*w*) mutations were created. As *y w* are both recessive markers on the *X* chromosome, larvae from *y w; Blm* mothers will appear phenotypically wild-type when crossed to wild-type males; alternatively, male larvae are hemizygous and will appear phenotypically *y w*. In larval stages, *yellow* mutants exhibit brown mouth hooks (as opposed to black) and *white* mutants exhibit clear Malpighian tubules (as opposed to white) (Lindsley and Zimm 1992). These newly created stocks not only make sex determination much more efficient relative to PCR, but also do not require larval sacrifice. Therefore, we will be able to follow *y w*; *Blm* mutant progeny from early larval stages until death or eclosion to better pinpoint lethality throughout development based on sex.

Additionally, two newly created transgenic constructs may help elucidate when and where Blm localizes in the early embryo. *P{Blm::mCherry-Blm^{+}}* and *P{Blm::mCherry-Blm^{D3}}* express an *mCherry* tagged wild-type and helicase dead *D3* mutant under control of the endogenous *Blm* promoter, respectively (see Materials and Methods). As the *D3* allele shows a severe reduction in SDSA relative to other heteroallelic combinations, McVey *et al.* hypothesized that *D3* is semidominant for SDSA repair defects (McVey *et al.* 2007) and may therefore become stuck at repetitive elements found within heterochromatin and resulting anaphase bridges. Co-staining for satellite sequences (such as the 359-bp repeat) using Oligopaints will allow us to determine if Blm colocalizes to these sequences, and may provide evidence that Blm is required to deal with replication challenges resulting from stalled replication forks or secondary DNA structures arising from these repetitive elements in the early embryo.

As Blm appears to play a zygotic role in preventing lethality throughout development, these newly created constructs can also be used to analyze the degradation of maternally-loaded Blm at NC 14. Utilizing antibodies against mCherry, the concentration of maternally-loaded *P{Blm::mCherry-Blm^{+}}* can be analyzed throughout embryogenesis via Western blot. Confirming maternal degradation at the switch between maternal-to-zygotic switch gene transcription (MBT) would provide further evidence supporting a zygotic role for Blm in developmental lethality.

Lastly, Dr. Eric Stoffregen created *Blm* mutant stocks carrying RFP-tagged H2AV, a variant of histone H2A, to follow nuclear defects during early embryonic stages. Using IF live imaging techniques, we will be able to determine if the nuclear fallout phenotype seen in the later syncytial blastoderm are daughter nuclei originating from a single, earlier nuclear defect, rather than an inwards collapse of nearby, non-defective nuclei. These results may suggest that the prolonged lethality seen in *Blm* mutants is due to earlier nuclear defects, and why a zygotic role for Blm may be important throughout development.

Materials and Methods

Drosophila stocks and genetics

Flies were maintained at 25˚C on standard medium. The Reaper Assay utilizes the GAL4/UASp system to express the apoptotic activating Reaper protein, thus activating cell death when expressed (Wang 1999). To obtain only female *blm^{N1} / blm^{D2}* progeny to be used in all experiments, *w P{w^{+} sxl::eGFP} ; P{GawB (GAL4)}^{h1J3} blm^{N1} / TM3 Sb Ser P{twist::GAL4}* females were crossed to *w P{w^{+} sxl::eGFP} / P {w+ UASp::rpr} ; blm^{D2} Sb / TMB Hu Tb e P{w+ UASp::rpr)* males. Progeny surviving to

adulthood are all female with the genotype *w P{w⁺ sxl::eGFP} ; P{GawB (GAL4)}^{h1J3} blm^{N1} / blm^{D2} Sb*, as all other sibling classes are lethal due to *rpr* expression in the early embryo or homozygous lethal *Sb*. Males used in sex bias and pharate adult experiments were isogenized *w^{1118}* and *w ; blm^{N1} / TM6B Hu Tb e.*

Females to be used in future larval sex determination were created by crossing *w / y w ; st blm^{D2} / TM3 Sb* females to *y w ; blm^{N1} / TM6B Hu ry* males and *w / y w ; st blm^{D2} / TM6B Hu ry* females to *y w ; blm^{N1} / TM3 Sb* males. Resulting stocks are *y w* ; *st blm^{D2} / TM6B Hu ry*, *y w* ; *st blm^{D2} / TM3 Sb, y w ; blm^{N1} / TM6B Hu ry,* and *y w ; blm^{N1} / TM3 Sb*.

Immunofluorescence

To determine temporal H3K9me2 localization, virgin *w^{1118}* or *blm^{N1} / blm^{D2}* females were mated to *w^{1118}* males. Embryos were collected on grape-agar plates for 4 hours, followed by dechorionation with 50% bleach, devitellenization with heptane, and fixed with 7% formaldehyde. Fixed embryos were incubated in 0.3% PBS-Triton® X-100 (ThermoFisher Scientific, Waltham, MA) for 30 minutes and blocked with 5% NGS (Sigma-Aldrich Corp., St. Louis, MO) for 1 hour. H3K9me2 primary staining utilized α-H3k9me2 (ab1220) (Abcam, Cambridge, MA) at a 1:400 concentration, followed by secondary staining with Alexa Fluor® 555 (ThermoFisher Scientific, Waltham, MA) at a 1:500 concentration. Both primary and secondary staining incubated at 4°C overnight and were subsequently washed 6 times for 20 minutes each. Following antibody staining, embryos were stained with 1 µg/ml DAPI and mounted with Fluoromount-G (ThermoFisher Scientific, Waltham, MA). Images were taken with ZEISS ZEN Software

on a Zeiss LSM710 confocal laser scanning microscope (Carl Zeiss, Inc., Thornwood, NY).

To determine early embryonic sex bias, virgin *sxl::eGFP* or blm^{N1} / blm^{D2} females were mated to w^{1118} males. Embryos were collected on grape agar plates for 2 hours and aged 6 hours, and fixed using the protocol described above. To increase eGFP signal in the embryo, primary staining utilized α-GFP (ab290) (Abcam, Cambridge, MA) at a 1:200 concentration, followed by secondary staining with Alexa Fluor® 594 (ThermoFisher Scientific, Waltham, MA) at a 1:500 concentration. Following antibody staining, embryos were stained with 1 µg/ml DAPI and mounted with Fluoromount-G (ThermoFisher Scientific, Waltham, MA). Images were taken as described above.

Studies of embryonic death

Virgin w^{1118} or blm^{N1} / blm^{D2} females were mated to w^{1118} males. Embryos were collected on grape-agar plates for 3 hours and allowed to age to the appropriate time point. Embryos were fixed, stained with DAPI, and imaged using the protocol described above.

Pharate lethality experiments

Virgin w^{1118} or blm^{N1} / blm^{D2} females were mated to w^{1118} males or blm^{N1}/*TM6B* males. Parents were flipped after 3 days and resulting progeny was scored over 12 days to ensure developmentally delayed adults were not scored as pharate. DNA was collected from pharate adults 2 days after all sibling eclosion and sex was determined via primers targeting the *Y* chromosome (5'-CTTCAAGGACTAAATGCGCAACT-3' and 5'-AAGGCTCCAACCTATTCGTATGT-3').

REFERENCES

Abdu, U., Brodsky, M., and Schüpbach, T. (2002). Activation of a Meiotic Checkpoint during *Drosophila* Oogenesis Regulates the Translation of Gurken through Chk2/Mnk. Curr. Biol. *12*, 1645–1651.

Ables, E.T. (2015). *Drosophila* Oocytes as a Model for Understanding Meiosis: An Educational Primer to Accompany “Corolla Is a Novel Protein That Contributes to the Architecture of the Synaptonemal Complex of Drosophila.” Genetics *199*, 17 23.

Adams, M.D., McVey, M., and Sekelsky, J.J. (2003) *Drosophila* BLM in double-strand break repair by synthesis-dependent strand annealing. Science *299*, 265–267.

Alderton, G.K., Joenje, H., Varon, R., Børglum, A.D., Jeggo, P.A., and O’Driscoll, M. (2004). Seckel syndrome exhibits cellular features demonstrating defects in the ATR-signalling pathway. Hum. Mol. Genet. *13*, 3127–3138.

Allers, T., and Lichten, M. (2001). Differential timing and control of noncrossover and crossover recombination during meiosis. Cell *106*, 47–57.

Andersen, S.L., and Sekelsky, J.J. (2010). Meiotic versus mitotic recombination: Two different routes for double-strand break repair. BioEssays *32*, 1058–1066.

Andersen, S.L., Kuo, H.K., Savukoski, D., Brodsky, M.H., and Sekelsky, J. (2011). Three structure-selective endonucleases are essential in the absence of BLM helicase in *Drosophila*. PLoS Genet. *7*, e1002315.

Ashburner, M., Golic, K.G., and Hawley, R.S. (2005). Drosophila: A Laboratory Handbook (Cold Spring Harbor, N.Y., Cold Spring Harbor Laboratory).

Baker, W.K. (1958) Crossing over in heterochromatin. Am. Nat. *92*, 59-60.

Baker, B.S., and Carpenter, A.T.C. (1972). Genetic Analysis of Sex Chromosomal Meiotic Mutants in *Drosophila melanogaster*. Genetics *71*, 255–286.

Baker, B.S., Boyd, J.B., Carpenter, A.T., Green, M.M., Nguyen, T.D., Ripoll, P., and Smith, P.D. (1976). Genetic controls of meiotic recombination and somatic DNA metabolism in *Drosophila melanogaster*. Proc. Natl. Acad. Sci. U.S.A. *73*, 4140–4144.

Bannister, A.J., Zegerman, P., Partridge, J.F., Miska, E.A., Thomas, J.O., Allshire, R.C., Kouzarides, T. (2001). Selective recognition of methylated lysine 9 on histone H3 by the HP1 chromo domain. Nature *410*, 120-124.

Ball, H.L., Myers, J.S. and Cortez, D. (2005). ATRIP binding to replication protein A-single-stranded DNA promotes ATR-ATRIP localization but is dispensable for Chk1 phosphorylation. Mol. Biol. Cell *16*, 2372-2381.

Beadle, G.W. (1932). A Possible Influence of the Spindle Fiber on Crossing-Over in *Drosophila*. Proc. Natl. Acad. Sci. U.S.A. *18*, 160–165.

Berchowitz, L.E., Francis, K.E., Bey, A.L., and Copenhaver, G.P. (2007). The role of AtMUS81 in interference-insensitive crossovers in *A. thaliana*. PLoS Genet *3*, e132.

Berchowitz, L.E., and Copenhaver, G.P. (2010). Genetic Interference: Don't Stand So Close to Me. Curr. Genomics *11*, 91–102.

Bergerat, A., de Massy, B., Gadelle, D., Varoutas, P.C., Nicolas, A., and Forterre, P. (1997) An atypical topoisomerase II from Archaea with implications for meiotic recombination. Nature *386*, 414-417.

Bishop, D.K. (1994). RecA homologs Dmc1 and Rad51 interact to form multiple nuclear complexes prior to meiotic chromosome synapsis. Cell *79*, 1081–1092.

Blanton, H. L., Radford S. J., Mcmahan S., Kearney H. M., Ibrahim J. G. *et al.* (2005) REC, *Drosophila* MCM8, drives formation of meiotic crossovers. PLoS Genet. *1*, e40.

Blumenthal, A.B., Kriegstein, H.J., and Hogness, D.S. (1974). The units of DNA replication in *Drosophila melanogaster* chromosomes. Cold Spring Harb. Symp. Quant. Biol. *38*, 205–223.

Bosotti, R., Isacchi, A., and Sonnhammer, E.L.L. (2000). FAT: A novel domain in PIK-related kinases. Trends Biochem. Sci. *25*, 225–227.

Boyd, J.B., Golino, M.D., Nguyen, T.D., and Green, M. M. (1976). Isolation and characterization of X-linked mutants of *Drosophila* melanogaster which are sensitive to mutagens. Genetics *84*, 485-506.

Boyd, J.B., Golino, M.D. Shaw, K.E.S, Osgood, C.J., and Green, M.M. (1981) Third-Chromosome Mutagen-Sensitive Mutants of *Drosophila melanogaster*. Genetics *97*, 607-623.

Bridges, C.B. (1935). Salivary chromosome maps with a key to the banding of the chromosomes of *Drosophila melanogaster*. J. Hered. *26*, 60-64.

Brodsky, M.H., Sekelsky, J., Tsang, G., Hawley, R.S., and Rubin, G.M. (2000). *mus304* encodes a novel DNA damage checkpoint protein required during *Drosophila* development. Genes Dev. *14*, 666-678.

Brodsky, M.H., Weinert, B.T., Tsang, G., Rong, Y.S., McGinnis, N.M., Golic, K.G., Rio, D.C., and Rubin, G.M. (2004). *Drosophila melanogaster* MNK/Chk2 and p53 regulate multiple DNA repair and apoptotic pathways following DNA damage. Mol. Cell. Biol. *24*, 1219–1231.

Brosh, R.M., Jr., Li, J.L., Kenny, M.K., Karow, J.K., Cooper, M.P. *et al.* (2000) Replication protein A physically interacts with the Bloom's syndrome protein and stimulates its helicase activity. J. Biol. Chem. *275*, 23500–23508.

Brown, M.S. (1940) Chiasma formation in the *bobbed* region of the X chromosome of *Drosophila melanogaster*. Studies in the Genetics of *Drosophila*, Univ. Texas Publ. No. *4032*, 65-70.

Bugreev, D.V., Yu, X., Egelman, E.H., Mazin, A.V. (2007). Novel pro- and anti-recombination activities of the Bloom's syndrome helicase. Genes Dev. *21*, 3085-3094.

Byzmek, M., Thayer, N.H., Oh, S.D., Kleckner, N., Hunter, N. (2010) Double Holliday Junctions are Intermediates of DNA Break Repair. Nature *464*, 937-941.

Carballo, J.A., Johnson, A.L., Sedgwick, S.G., and Cha, R.S. (2008). Phosphorylation of the Axial Element Protein Hop1 by Mec1/Tel1 Ensures Meiotic Interhomolog Recombination. Cell *132*, 758–770.

Carpenter, A.T.C. (1979). Recombination Nodules and Synaptonemal Complex in Recombination-Defective Females of *Drosophila melanogaster*. Chromosoma *75*, 259-292.

Choo, K.H.A. (1998). Why Is the Centromere So Cold? Genome Research *8*, 81–82.

Cloud, V., Chan, Y.L., Grubb, J., Budke, B., Bishop, D.K. (2012) Rad51 is an accessory factor for Dmc1-mediated joint molecule formation during meiosis. Science *337*, 1222-1225.

Comeron, J.M., Ratnappan, R., and Bailin, S. (2012). The Many Landscapes of Recombination in *Drosophila melanogaster*. PLoS Genet. *8*, 33–35.

Cooper, T.J., Wardell, K., Garcia, V., and Neale, M.J. (2014). Homeostatic regulation of meiotic DSB formation by ATM/ATR. Exp. Cell Res. *329*, 124–131.

Cooper, T.J., Garcia, V., and Neale, M.J. (2016). Meiotic DSB patterning: A multifaceted process. Cell Cycle *15*, 13–21.

Copenhaver, G.P., Housworth, E.A., and Stahl, F.W. (2002). Crossover interference in Arabidopsis. Genetics *160*, 1631-1639.

Darlington, C.D., and Dark, S.O.S. (1932). The origin and behaviour of chiasmata, II. Stenobothrus parallelus. Cytologia (Tokyo) *3*, 169–185.

de los Santos, T., Hunter, N., Lee, C., Larkin, B., Loidl, J., and Hollingsworth, N.M. (2003). The Mus81/Mms4 endonuclease acts independently of double-Holliday junction resolution to promote a distinct subset of crossovers during meiosis in budding yeast. Genetics *164*, 81-94.

De Muyt, A., Jessop, L., Kolar, E., Sourirajan, A., Chen, J., Dayani, Y., and Lichten, M. (2012). BLM helicase ortholog Sgs1 is a central regulator of meiotic recombination intermediate metabolism. Mol. Cell *46*, 43-53.

Dobson, M.J., Pearlman, R.E., Karaiskakis, A., Spyropoulos, B., Moens, P.B. (1994) Synaptonemal complex proteins: occurrence, epitope mapping and chromosome disjunction. J Cell Sci. *107*, 2749-2760.

Duronio, R.J. (2012). Developing S-phase control. Genes Dev. *26*, 746–750.

Elgin, S.C. and Reuter, G. (2013). Position-effect variegation, heterochromatin formation, and gene silencing in *Drosophila*. Cold Spring Harb Perspect Biol. *5*, a017780.

Ellis, N.A., Groden, J., Ye, T.Z., Straughen, J., Lennon, D.J., Ciocci, S., Proytcheva, M., German, J. (1995) The Bloom's syndrome gene product is homologous to RecQ helicases. Cell *83*, 655-666.

Foe, V.E., Alberts, B.M. (1983) Studies of nuclear and cytoplasmic behaviour during the five mitotic cycles that precede gastrulation in *Drosophila* embryogenesis. J Cell Sci. *61*, 31-70.

Garcia, V., Phelps, S.E., Gray, S., Neale, M.J. (2011). Bidirectional resection of DNA double-strand breaks by Mre11 and Exo1. Nature *479*, 241-244.

Garner, M., Van Kreeveld, S., and Su, T.T. (2001). mei-41 and bub1 block mitosis at two distinct steps in response to incomplete DNA replication in *Drosophila* embryos. Curr. Biol. *11*, 1595–1599.

Gaymes, T.J., North, P.S., Brady, N., Hickson, I.D., Mufti, G.J. and Rassool, F.V. (2002) Increased error-prone non homologous DNA end-joining--a proposed mechanism of chromosomal instability in Bloom's syndrome. Oncogene *21*, 2522-2533.

German, J. (1993). Bloom syndrome: a mendelian prototype of somatic mutational disease. Medicine (Baltimore) *72*, 393-406.

Ghabrial, A., Ray, R.P., and Schüpbach, T. (1998). *okra* and *spindle-B* encode components of the RAD52 DNA repair pathway and affect meiosis and patterning in *Drosophila* oogenesis. Genes Dev. *12*, 2711–2723.

Ghabiral, A., and Schüpbach, T. (1999). Activation of a meiotic checkpoint regulates translation of Gurken during *Drosophila* oogenesis. Nat. Cell Biol. *1*, 354–357.

Gonzalez-Barrera, S., Cortes-Ledesma, F., Wellinger, R.E., Aguilera, A., Cortes-Ledesma, F., Wellinger, R.E., Aguilera, A., Wellinger, R.E., Aguilera, A., Aguilera, A. (2003) Equal sister chromatid exchange is a major mechanism of double-strand break repair in yeast. Mol. Cell. *11*, 1661–1671.

Grushcow, J.M., Holzen, T.M., Park, K.J., Weinert, T., Lichten, M., and Bishop, D.K. (1999). Saccharomyces cerevisiae checkpoint genes MEC1, RAD17 and RAD24 are required for normal meiotic recombination partner choice. Genetics *153*, 607–620.

Hari, K.L., Santerre, A., Sekelsky, J.J., McKim, K.S., Boyd, J.B., and Hawley, S.R. (1995). The mei-41 gene of D. melanogaster is a structural and functional homolog of the human ataxia telangiectasia gene. Cell *82*, 815–821.

Hartmann, M.A. and Sekelsky, J. (2017) The absence of crossovers on chromosome 4 in *Drosophila melanogaster*: Imperfection or interesting exception? Fly (Austin) 1–7.

Hatkevich, T., Kohl, K.P., McMahan, S., Hartmann, M.A., Williams, A.M., and Sekelsky, J. (2017). Bloom Syndrome Helicase Promotes Meiotic Crossover Patterning and Homolog Disjunction. Curr. Biol. *27*, 96-102.

Hatkevich, T., and Sekelsky, J. (2017). Bloom Syndrome Helicase in Meiosis: An Anti-Crossover Protein with Pro-Crossover Functions. BioEssays. *39*, 1700073. doi:10.1002/bies.201700073

Hawley, R.S. (1988) Exchange and chromosomal segregation in eukaryotes. In Genetic Recombination, pp. 497–527.

Hawley, R.S. (1993). Meiosis as an "M" thing: twenty-five years of meiotic mutants in *Drosophila*. Genetics *135*, 613-618.

Hickson, I.D. (2003). RecQ helicases: caretakers of the genome. Nat. Rev. Cancer *3*, 169-178.

Holliday, R. (1964). A mechanism for gene conversion in fungi. Genetical Research *78*, 282-304.

Hollingsworth, N.M., Ponte, L., Halsey, C. (1995) *MSH5*, a novel MutS homolog, facilitates meiotic reciprocal recombination between homologs in *Saccharomyces cerevisiae* but not mismatch repair. Genes Dev. 9, 1728-1739.

Holsclaw, J. K. and Sekelsky J. (2017) Annealing of Complementary DNA Sequences During Double-Strand Break Repair in *Drosophila* Is Mediated by the Ortholog of SMARCAL1. Genetics *206*, 467–480.

Hu, Y., Lu, X., Barnes, E., Yan, M., Lou, H., et al. (2005). Recql5 and BLM RecQ DNA helicases have nonredundant roles in suppressing crossovers. Mol. Cell. Biol. *25*, 3431–3442.

Hunter, N., Kleckner, N. (2001). The single-end invasion: an asymmetric intermediate at the double-strand break to double-Holliday junction transition of meiotic recombination. Cell *106*, 59-70.

Hunter, N., Flemming, W., and Boveri, T. (2015). Meiotic Recombination: The Essence of Heredity. Cold Spring Harb. Perspect. Biol. *7*, a016618

Jaklevic, B.R., and Su, T.T. (2004). Relative Contribution of DNA Repair, Cell Cycle Checkpoints, and Cell Death to Survival after DNA Damage in *Drosophila* Larvae. Curr. Biol. *14*, 23–32.

Jang, J.K., Sherizen, D.E., Bhagat, R., Manheim, E.A., McKim, K.S. (2003) Relationship of DNA double-strand breaks to synapsis in *Drosophila*. J. Cell Sci. *116*, 3069-3077.

Jennings, B.H. (2011). *Drosophila* - a versatile model in biology & medicine. Mater. Today *14*, 190–195.

Joyce, E.F., Pedersen, M., Tiong, S., White-Brown, S.K., Paul, A., Campbell, S.D., and McKim, K.S. (2011). *Drosophila* ATM and ATR have distinct activities in the regulation of meiotic DNA damage and repair. J. Cell Biol. *195*, 359–367.

Kadyk, L.C., Hartwell, L.H. (1992) Sister chromatids are preferred over homologs as substrates for recombinational repair in Saccharomyces cerevisiae. Genetics *132,* 387-402.

Karow, J.K., Chakraverty, R.K., Hickson, I.D. (1997) The Bloom's syndrome gene product is a 3'-5' DNA helicase. J Biol. Chem. *272*, 30611-30614.

Karow, J.K., Constantinou, A., Li, J.L., West, S.C., Hickson, I.D. (2000) The Bloom's syndrome gene product promotes branch migration of holliday junctions. Proc. Natl. Acad. Sci. U.S.A. *97*, 6504-6508.

Keegan, K.S., Holtzman, D.A., Plug, A.W., Christenson, E.R., Brainerd, E.E., Flaggs, G., Bentley, N.J., Taylor, E.M., Meyn, M.S., Moss, S.B., et al. (1996). The Atr and Atm protein kinases associate with different sites along meiotically pairing chromosomes. Genes Dev. *10*, 2423–2437.

Keeney, S., Giroux, C.N., Kleckner, N. (1997). Meiosis-Specific DNA Double-Strand Breaks Are Catalyzed by Spo11, a Member of a Widely Conserved Protein Family. Cell *88*, 375-384.

Keeney, S. (2008). Spo11 and the Formation of DNA Double-Strand Breaks in Meiosis. Genome Dyn. Stab. *2*, 81-123.

Kelly, K.O., Dernburg, A.F., Stanfield, G.M., Villeneuve, A.M. (2000) *Caenorhabditis elegans msh-5* is required for both normal and radiation-induced meiotic crossing over but not for completion of meiosis. Genetics *156*, 617-630.

Kleckner, N., Zickler, D., Jones, G.H., Dekker, J., Padmore, R., Henle, J., Hutchinson, J. (2004). A mechanical basis for chromosome function. Proc. Natl. Acad. Sci. U.S.A. *101*, 12592–12597.

Koehler, K.E., Boulton, C.L., Collins, H.E., French, R.L., Herman, K.C., Lacefield, S.M., Madden, L.D., Schuetz, C.D., and Hawlet, S.R. (1996). Spontaneous X chromosome MI and MII nondisjunction events in *Drosophila melanogaster* oocytes have different recombinational histories. Nat Genet. *14*, 353–356.

Kohl, K.P., Jones, C.D., and Sekelsky, J. (2012). Evolution of an MCM complex in flies that promotes meiotic crossovers by blocking BLM helicase. Science *338*, 1363-1365.

Kohl, K.P., and Sekelsky, J.J. (2013). Meiotic and Mitotic Recombination in Meiosis. Genetics *194*, 327–334.

Kriegstein, H.J., Hogness, D.S. (1974). Mechanism of DNA replication in *Drosophila* chromosomes: structure of replication forks and evidence for bidirectionality. Proc Natl Acad Sci USA *71*, 135-139.

Kusano, K., Johnson-Schlitz, D.M., Engels, W.R. (2001) Sterility of *Drosophila* with mutations in the Bloom syndrome gene--complementation by *Ku70*. Science *291*, 2600-2602.

Lachner, M., O'Carroll, D., Rea, S., Mechtler, K., Jenuwein, T. (2001) Methylation of histone H3 lysine 9 creates a binding site for HP1 proteins. Nature *410*, 116-120.

Lake, C.M., and Hawley, R.S. (2012). The molecular control of meiotic chromosomal behavior: events in early meiotic prophase in *Drosophila* oocytes. Annu. Rev. Physiol. *74*, 425–451.

Lamb, N.E., Freeman, S.B., Savage-Austin, A., Pettay, D., Taft, L., Hersey, J., Gu, Y., Shen, J., Saker, D., May, K.M., et al. (1996). Susceptible chiasmate configurations of chromosome 21 predispose to non-disjunction in both maternal meiosis I and meiosis II. Nat. Genet. *14*, 400–405.

LaRocque, J.R., Jaklevic, B., Tin, T.S., and Sekelsky, J. (2007). *Drosophila* ATR in double-strand break repair. Genetics *175*, 1023–1033.

Laurençon, A., Purdy, A., Sekelsky, J., Hawley, R.S., and Su, T.T. (2003). Phenotypic analysis of separation-of-function alleles of MEI-41, *Drosophila* ATM/ATR. Genetics *164*, 589–601.

Lindsley, D.L. and Zimm, G.G. (1992). The genome of *Drosophila melanogaster*. Academic Press, La Jolla.

Li, X.Y., Harrison, M.M., Villalta, J.E., Kaplan, T., Eisen, M.B. (2014) Establishment of regions of genomic activity during the *Drosophila* maternal to zygotic transition. Elife *3*, e03737.

Liu, H., Jang, J.K., Kato, N., and McKim, K.S. (2002). mei-P22 encodes a chromosome-associated protein required for the initiation of meiotic recombination in *Drosophila* melanogaster. Genetics *162*, 245–258.

Lu, X., Liu, X, An, L., Zhang, W., Sun, J., Pei, H., Meng, H., Fan, Y, and Zhang, C. (2008) The *Arabidopsis MutS* homolog *AtMSH5* is required for normal meiosis. Cell Res *18*, 589–99.

MacQueen, A.J., and Hochwagen, A. (2011). Checkpoint mechanisms: The puppet masters of meiotic prophase. Trends Cell Biol. *21*, 393–400.

Manfrini, N., Guerini, I., Citterio, A., Lucchini, G., Longhese, M.P. (2010) Processing of meiotic DNA double strand breaks requires cyclin-dependent kinase and multiple nucleases. J. Biol. Chem. *285*, 11628-11637.

Manhart, C.M., Alani, E. (2016) Roles for mismatch repair family proteins in promoting meiotic crossing over. DNA Repair (Amst). *38*, 84-93.

Masrouha, N., Yang, L., Hijal, S., Larochelle, S., and Suter, B. (2003). The *Drosophila chk2* gene *loki* is essential for embryonic DNA double-strand-break checkpoints induced in S phase or G2. Genetics *163*, 973-982.

Marcon, E., and Moens, P.B. (2005). The evolution of meiosis: Recruitment and modification of somatic DNA-repair proteins. BioEssays *27*, 795–808.

Maréchal, A., and Zou, L. (2013). DNA damage sensing by the ATM and ATR kinases. Cold Spring Harb. Perspect. Biol. *5*, 1–17.

Martini, E., Diaz, R.L., Hunter, N., and Keeney, S. (2006). Crossover Homeostasis in Yeast Meiosis. Cell *126*, 285–295.

Mather, K. (1939) Crossing over and Heterochromatin in the X Chromosome of *Drosophila melanogaster*. Genetics *24*, 413–435.

McKim, K.S., Jang, J.K., Theurkauf, W.E., and Hawley, R.S. (1993) Mechanical basis of meiotic metaphase arrest. Nature *362*, 364–366.

McKim, K.S., Green-Marroquin, B.L., Sekelsky, J.J., Chin, G., Steinberg, C., Khodosh, R., and Hawley, R.S. (1998) Meiotic synapsis in the absence of recombination. Science *279*, 876–8.

McVey, M., Adams, M., Staeva-Vieira, E., and Sekelsky, J.J. (2004a). Evidence for multiple cycles of strand invasion during repair of double-strand gaps in *Drosophila*. Genetics *167*, 699–705.

McVey, M., Larocque, J.R., Adams, M.D., and Sekelsky, J.J. (2004b). Formation of deletions during double-strand break repair in *Drosophila* DmBlm mutants occurs after strand invasion. Proc. Natl. Acad. Sci. U.S.A. *101*, 15694–15699.

McVey, M., Andersen, S.L., Broze, Y., and Sekelsky, J. (2007). Multiple functions of *Drosophila* BLM helicase in maintenance of genome stability. Genetics *176*, 1979–1992.

Mehrotra, S., and McKim, K.S. (2006). Temporal analysis of meiotic DNA double-strand break formation and repair in *Drosophila* females. PLoS Genet. *2*, 1883–1897.

Miller, M.P., Amon, A., and Ünal, E. (2013). Meiosis I: When chromosomes undergo extreme makeover. Curr. Opin. Cell Biol. *25*, 687–696.

Miller, D.E., Smith, C.B., Kazemi, N.Y., Cockrell, A.J., Arvanitakis, A.V., Blumenstiel, J.P., Jaspersen, S.L., and Hawley, R.S. (2016) Whole-Genome Analysis of Individual Meiotic Events in *Drosophila melanogaster* Reveals That Non-crossover Gene Conversions Are Insensitive to Interference and the Centromere Effect. Genetics *203*, 159–171.

Mordes, D.A., and Cortez, D. (2008) Activation of ATR and related PIKKs. Cell Cycle *7*, 2809-2812.

Morgan, T.H. (1912). Complete linkage in the second chromosome of the male of *Drosophila*. Science *36*, 719-720.

Muller, H. J., and T. S. Painter. (1932) The differentiation of the sex chromosomes of *Drosophila* into genetically active and inert regions. *Z*. Induct. Abstammungs Vererbungsl. *62***,** 316-365.

Nagaoka, S.I., Hassold, T.J., and Hunt, P.A. (2012). Human aneuploidy: mechanisms and new insights into an age-old problem. Nat. Rev. Genet. *13*, 493–504.

Nagoshi, R.N. (2004). Oogenesis. In Encyclopedia of Entomology, pp. 1594–1598.

Nakayama, J., Rice, J.C., Strahl, B.D., Allis, C.D., Grewal, S.I. (2001) Role of histone H3 lysine 9 methylation in epigenetic control of heterochromatin assembly. Science *292*, 110-113.

Neale, M.J., Pan, J., Keeney, S. (2005). Endonucleolytic processing of covalent protein-linked DNA double-strand breaks. Nature *436*, 1053-1057.

O'Dor, E., Beck, S.A., Brock, H.W. (2006). Polycomb group mutants exhibit mitotic defects in syncytial cell cycles of *Drosophila* embryos. Dev Biol. *290*, 312-322.

O'Driscoll, M., Ruiz-Perez, V.L., Woods, C.G., Jeggo, P.A., and Goodship, J.A. (2003). A splicing mutation affecting expression of ataxia-telangiectasia and Rad3-related protein (ATR) results in Seckel syndrome. Nat. Genet. *33*, 497–501.

O'Farrell, P.H., Edgar, B.A., Lakich, D., Lehner, C.F. (1989). Directing cell division during development. Science *246*, 635-640.

O'Farrell, P.H., Stumpff, J., Su, T.T. (2004) Embryonic cleavage cycles: how is a mouse like a fly? Curr. Biol. *14*, 35-45.

Oikemus, S.R., Queiroz-Machado, J., Lai, K., McGinnis, N., Sunkel, C., and Brodsky, M.H. (2006). Epigenetic telomere protection by *Drosophila* DNA damage response pathways. PLoS Genet. *2*, 693–706.

Osborne, J.D. (1999). Crossing over in a T(1;4) translocation in *Drosophila melanogaster*. MS thesis (University of Alberta).

Owen, A.R. (1949). A possible interpretation of the apparent interference across the centromere found by Callan and Montalenti in Culex pipiens. Heredity (Edinb.) *3*, 357–367.

Pacheco, S., Maldonado-Linares, A., Marcet-Ortega, M., Rojas, C. *et al.* (2017). ATR is required to complete meiotic recombination in mice. bioRxiv 133744; doi: https://doi.org/10.1101/133744

Pedrazzi, G., Perrera, C., Blaser, H., Kuster, P., Marra, G., *et al.* (2001). Direct association of Bloom's syndrome gene product with the human mismatch repair protein MLH1. Nucleic Acids Res. *29*, 4378–4386.

Ralf, C., Hickson, I.D., and Wu, L. (2006) The Bloom's syndrome helicase can promote the regression of a model replication fork. J. Biol. Chem. *281*, 22839–22846.

Redfield, H. (1932) A Comparison of Triploid and Diploid Crossing over for Chromosome II of *Drosophila melanogaster*. Genetics *17*, 137–52.

Refolio, E., Cavero, S., Marcon, E., Freire, R., and San-Segundo, P.A. (2011). The Ddc2/ATRIP checkpoint protein monitors meiotic recombination intermediates. J. Cell Sci. *124*, 2488–2500.

Robert, T., Nore, A., Brun, C., Maffre, C., Crimi, B., Bourbon, H.M., and de Massy, B. (2016). The TopoVIB-Like protein family is required for meiotic DNA double-strand break formation. Science *351*, 943–949.

Roberts, P. A. (1965) Difference in the behavior of eu- and hetero-chromatin: crossing-over. Nature *205*, 725-726.

Ross-Macdonald, P., Roeder, G.S. (1994) Mutation of a meiosis-specific MutS homolog decreases crossing over but not mismatch correction. Cell *79*: 1069–1080.

Royou, A., Macias, H., and Sullivan, W. (2005). The *Drosophila* Grp/Chk1 DNA damage checkpoint controls entry into anaphase. Curr. Biol. *15*, 334-339.

Sanghavi, P., Laxani, S., Li X., Bullock, S.L., and Gonsalvez, G.B. (2013) Dynein Associates with *oskar* mRNPs and Is Required for Their Efficient Net Plus-End Localization in *Drosophila* Oocytes. PLoS One *8*, e80605.

Schüpbach, T., Roth, S. (1994) Dorsoventral patterning in *Drosophila* oogenesis. Curr Opin Genet Dev. *4*, 502-507.

Schütt, C. and Nöthiger, R. (2000). Structure, function and evolution of sex-determining systems in Dipteran insects. Development *127*, 667-677.

Schwacha, A., and Kleckner, N. (1994). Identification of joint molecules that form frequently between homologs but rarely between sister chromatids during yeast meiosis. Cell *76*, 51–63.

Sekelsky, J., McKim, K.S., Chin, G.M., and Hawley, R.S. (1995). The *Drosophila* meiotic recombination gene *mei-9* encodes a homologue of the yeast excision repair protein Rad1. Genetics *141*, 619-627.

Sengupta, S., Linke, S.P., Pedeux, R., Yang, Q., Farnsworth, J. et al. (2003) BLM helicase-dependent transport of p53 to sites of stalled DNA replication forks modulates homologous recombination. EMBO J. *22*, 1210–1222.

Sengupta, S., Robles, A.I., Linke, S.P., Sinogeeva, N.I., Zhang, R. et al. (2004). Functional interaction between BLM helicase and 53BP1 in a Chk1-mediated pathway during S-phase arrest. J. Cell Biol. *166,* 801–813.

Shanske, A., Caride, D.G., Menasse-Palmer, L., Bogdanow, A., and Marion, R.W. (1997). Central nervous system anomalies in Seckel syndrome: report of a new family and review of the literature. Am. J. Med. Genet. *70*, 155–158.

Shermoen, A.W., McCleland, M.L., and O'Farrell, P.H. (2010). Developmental control of late replication and S phase length. Curr. Biol. *20*, 2067–2077.

Shinohara A., Shinohara M. (2004) Roles of RecA homologues Rad51 and Dmc1 during meiotic recombination. Cytogenet Genome Res. *107*, 201–207.

Sibanda, B.L., Chirgadze, D.Y., and Blundell, T.L. (2010). Crystal Structure of DNA-PKcs Reveals a Large Open-Ring Cradle Comprised of HEAT Repeats. Nature *463*, 118–121.

Sibon, O.C.M., Laurençon, A., Hawley, R.S., and Theurkauf, W.E. (1999). The *Drosophila* ATM homologue Mei-41 has an essential checkpoint function at the midblastula transition. Curr. Biol. *9*, 302–312.

Smith, G.R., Boddy, M.N., Shanahan, P., and Russell, P. (2003). Fission yeast Mus81.Eme1 Holliday junction resolvase is required for meiotic crossing over but not for gene conversion. Genetics *165*, 2289-2293.

Song, Y.H., Mirey, G., Betson, M., Haber, D.A., and Settleman, J. (2004). The *Drosophila* ATM Ortholog, dATM, Mediates the Response to Ionizing Radiation and to Spontaneous DNA Damage during Development. Curr. Biol. *14*, 1354–1359.

Sonoda, E., Sasaki, M.S., Morrison, C., Yamaguchi-Iwai, Y., Takata, M., and Takeda, S. (1999) Sister Chromatid Exchanges Are Mediated by Homologous Recombination in Vertebrate Cells. Mol. Cell. Biol. *19*, 5166-5169.

Spradling, A.C. (1993) Germline cysts: communes that work. Cell *72*, 649-651.

Staeva-Vieira, E., Yoo, S., and Lehmann, R. (2003). An essential role of DmRad51/SpnA in DNA repair and meiotic checkpoint control. EMBO J *22*, 5863–5874.

Stevens, W.L. (1936) The analysis of interference. J Genet *32*, 51–64.

Sturtevant, A.H. (1913). The linear arrangement of six sex-linked factors in *Drosophila*, as shown by their mode of association. J. Exp. Zool. *14*, 43–59.

Sturtevant, A.H., Beadle, G.W. (1936) The of relations inversions in the X chromosomes of *Drosophila melanogaster* to crossing-over and disjunction. Genetics *28*, 554–604.

Sturtevant, A.H. (1951) A map of the fourth chromosome of *Drosophila melanogaster*, based on crossing over in triploid females. Proc. Natl. Acad. Sci. U.S.A. *37*, 405–407.

Su, T. T., Campbell, S. D., and O'Farrell, P. H. (1999). *Drosophila grapes*/CHK1 mutants are defective in cyclin proteolysis and coordination of mitotic events. Curr. Biol. *9*, 919-922.

Sun, H., Karow, J.K., Hickson, I.D., Maizels, N. (1998) The Bloom's syndrome helicase unwinds G4 DNA. J. Biol. Chem. *273*, 27587-27592.

Symington, L.S., and Gautier, J. (2011). Double-Strand Break End Resection and Repair Pathway Choice. Annu. Rev. Genet. *45*, 247–271.

Tachibana, A., Tatsumi, K., Masui, T. and Kato, T. (1996) Large deletions at the *HPRT* locus associated with the mutator phenotype in a Bloom's syndrome lymphoblastoid cell line. Mol Carcinog. *17*, 41-47.

Tanaka, A., Weinel, S., Nagy, N., O'Driscoll, M., Lai-Cheong, J.E., Kulp-Shorten, C.L., Knable, A., Carpenter, G., Fisher, S.A., Hiragun, M., et al. (2012). Germline mutation in ATR in autosomal- dominant oropharyngeal cancer syndrome. Am. J. Hum. Genet. *90*, 511–517.

Thompson, J., Graham, P., Schedl, P., Pulak, R., and Road, W. (2004). Sex-specific GFP-expression in *Drosophila* embryos and sorting by COPAS^{TM} flow cytometry technique. In 45th Annual *Drosophila* Research Conference, pp. 1–4.

Trowbridge, K., McKim, K., Brill, S., and Sekelsky, J. (2007) Synthetic lethality in the absence of the *Drosophila* MUS81 endonuclease and the DmBlm helicase is associated with elevated apoptosis. Genetics *176*, 1993–2001.

van Brabant, A.J., Ye, T., Sanz, M., German, I.J., Ellis, N.A., and Holloman, W.K. (2000) Binding and melting of D-loops by the Bloom syndrome helicase. Biochemistry *39*, 14617-14625.

Villeneuve, A.M., Hillers, K.J. (2001) Whence meiosis? Cell *106*, 647-650.

Vincenten, N., Kuhl, L.M., Lam, I., Oke, A., Kerr, A.R.W., Hochwagen, A., Fung, J., Keeney, S., Vader, G., and Marston, A.L. (2015). The kinetochore prevents centromere-proximal crossover recombination during meiosis. eLife *4*, 1–25.

von Stetina, J.R., and Orr-Weaver, T.L. (2011). Developmental control of oocyte maturation and egg activation in metazoan models. Cold Spring Harb. Perspect. Biol. *3*, 1–19.

Wang, S., Zickler, D., Kleckner, N., and Zhang, L. (2015). Meiotic crossover patterns: Obligatory crossover, interference and homeostasis in a single process. Cell Cycle *14,* 305–314.

Weinstein, A. (1936). The theory of multiple-strand crossing over. Genetics *21*, 155–199.

Weinstein, A. (1958). The geometry and mechanics of crossing over. Cold Spring Harb. Symp. Quant. Biol. *23*, 177–96.

Wu, L., Davies, S.L., Levitt, N.C., and Hickson, I.D. (2001). Potential role for the BLM helicase in recombinational repair via a conserved interaction with RAD51. J. Biol. Chem. *276*, 19375-19381.

Xie, T., (2013) Control of germline stem cell self-renewal and differentiation in the *Drosophila* ovary: concerted actions of niche signals and intrinsic factors. Wiley Interdiscip. Rev. Dev. Biol. *2*, 261–273.

Yamamoto, M., Miklos, G.L.G. (1978) Genetic studies on heterochromatin in *Drosophila melanogaster* and their implications for the functions of satellite DNA. Chromosoma *66*, 71-98.

Yıldız, Ö., Majumder S., Kramer B. C., and Sekelsky, J. (2002) *Drosophila* MUS312 interacts with the nucleotide excision repair endonuclease MEI-9 to generate meiotic crossovers. Mol. Cell *10*, 1503-1509.

Yu, K. R., Saint, R. B., and Sullivan, W. (2000). The Grapes checkpoint coordinates nuclear envelope breakdown and chromosome condensation. Nat. Cell. Biol. *2*, 609-615.

Yuan, K. and O'Farrell, P.H. (2016). TALE-light imaging reveals maternally guided, H3K9me2/3-independent emergence of functional heterochromatin in *Drosophila* embryos. Genes Dev. *30*, 579-593.

Zakharyevich, K., Tang, S., Ma, Y., and Hunter, N. (2012). Delineation of joint molecule resolution pathways in meiosis identifies a crossover-specific resolvase. Cell *149*, 334–347.

Zalevsky, J., MacQueen A.J., Duffy, J.B., Kemphues, K.J., Villeneuve, A.M. (1999) Crossing over during *Caenorhabditis elegans* meiosis requires a conserved MutS-based pathway that is partially dispensable in budding yeast. Genetics *153*, 1271-1283.

Zeng, Y., Li, H., Schweppe N. M., Hawley R. S., and Gilliland, W. D. (2010) Statistical analysis of nondisjunction assays in *Drosophila*. Genetics *186*, 505-513.

Zhang, L., Liang, Z., Hutchinson, J., and Kleckner, N. (2014). Crossover Patterning by the Beam-Film Model: Analysis and Implications. PLoS Genet. *10*, e1004042.

Zhang, L., Wang, S., Yin, S., Hong, S., Kim, K.P., and Kleckner, N. (2014). Topoisomerase II mediates meiotic crossover interference. Nature *511*, 1–21.